

Review

Open Access



# Leveraging novel microwave techniques for tailoring the microstructure of energy storage materials

Yongfei You<sup>#</sup>, Guangyu Fang<sup>#</sup>, Miao Fan<sup>#</sup>, Jiayue Guo, Qingxiang Li, Jun Wan 

State Key Laboratory of New Textile Materials and Advanced Processing Technologies, Hubei Key Laboratory of Biomass Fibers and Eco-Dyeing & Finishing, Wuhan Textile University, Wuhan 430200, Hubei, China.

<sup>#</sup>Authors contributed equally.

**Correspondence to:** Prof. Jun Wan, State Key Laboratory of New Textile Materials and Advanced Processing Technologies, Wuhan Textile University, 1 Sunshine Avenue, Jiangxia District, Wuhan 430200, Hubei, China. E-mail: wanj@wtu.edu.cn

**How to cite this article:** You Y, Fang G, Fan M, Guo J, Li Q, Wan J. Leveraging novel microwave techniques for tailoring the microstructure of energy storage materials. *Microstructures* 2024;4:2024035. <https://dx.doi.org/10.20517/microstructures.2023.86>

**Received:** 10 Dec 2023 **First Decision:** 19 Jan 2024 **Revised:** 27 Jan 2024 **Accepted:** 8 Feb 2024 **Published:** 3 Jun 2024

**Academic Editor:** Jianfeng Mao **Copy Editor:** Fangyuan Liu **Production Editor:** Fangyuan Liu

## Abstract

In the dynamic landscape of energy storage materials, the demand for efficient microstructural engineering has surged, driven by the imperative to seamlessly integrate renewable energy. Traditional material preparation methods encounter challenges such as poor controllability, high costs, and stringent operational conditions. The advent of microwave techniques heralds a transformative shift, offering rapid responses, high-temperature energy, and superior controllability. This review critically examines the nuanced applications of microwave technology in tailoring the microstructure of energy storage materials, emphasizing its pivotal role in the energy paradigm and addressing challenges posed by conventional methods. Notably, non-liquid-phase advanced microwave technology holds promise for introducing novel models and discoveries compared to traditional liquid-phase microwave methods. The ensuing discussion explores the profound impact of advanced microwave strategies on microstructural engineering, highlighting discernible advantages in optimizing performance for energy storage applications. Various applications of advanced microwave techniques in this domain are comprehensively discussed, providing a forward-looking perspective on their untapped potential to propel transformative strides in renewable energy research. This review offers insights into the promising future of leveraging microwaves for tailoring the microstructure of energy storage materials.

**Keywords:** Microwave, microstructure, energy storage, metal-ion battery, supercapacitor



© The Author(s) 2024. **Open Access** This article is licensed under a Creative Commons Attribution 4.0 International License (<https://creativecommons.org/licenses/by/4.0/>), which permits unrestricted use, sharing, adaptation, distribution and reproduction in any medium or format, for any purpose, even commercially, as long as you give appropriate credit to the original author(s) and the source, provide a link to the Creative Commons license, and indicate if changes were made.



## INTRODUCTION

In the context of rapid societal advancement, the pressing need for energy storage technologies has become increasingly evident<sup>[1,2]</sup>. Currently, fossil fuels, including coal, natural gas, and oil, contribute to over 80% of the world's energy consumption. Extensively using these resources results in significant carbon dioxide emissions, contributing substantially to air pollution and climate change<sup>[3,4]</sup>. This reality underscores the urgent requirement for a transition to clean, renewable energy sources, specifically emphasizing solar and wind energy technologies<sup>[5-7]</sup>. However, the intermittent and unpredictable nature of these renewable energies poses a significant limitation, emphasizing the critical role of efficient energy storage systems<sup>[8,9]</sup>. Consequently, developing effective and environmentally friendly energy storage technologies and devices has become imperative. In this domain, batteries and supercapacitors have garnered substantial attention from researchers due to their remarkable energy and power densities, enduring cycle stability, broad operating temperature ranges, and environmentally friendly attributes<sup>[10]</sup>. The effectiveness of batteries and supercapacitors is intricately tied to the microstructure and chemical characteristics of their electrode materials<sup>[11-14]</sup>. Therefore, the research focus has shifted towards developing electrode materials featuring optimal structures, high reversibility, superior rate capabilities, electrochemical stability, and extended cycle life, representing a critical research priority.

Despite the availability of various methods for synthesizing electrode materials, such as chemical vapor deposition (CVD)<sup>[15]</sup>, electrochemical exfoliation<sup>[16]</sup>, spray pyrolysis<sup>[17]</sup>, and solvothermal techniques<sup>[18]</sup>, these approaches often encounter challenges, including high reaction temperatures, prolonged reaction durations, complex multi-step processes, scalability issues, and limited yields. These limitations impede their widespread application potential. In contrast, the liquid-phase microwave-assisted synthesis method distinguishes itself with notable advantages such as rapid, uniform heating, higher yields, and enhanced repeatability<sup>[19,20]</sup>. However, its effectiveness is somewhat constrained by its solvent dependence, limiting its versatility in synthesizing diverse materials. Specific materials may exhibit instability or poor solubility in certain solvents, thus restricting the extensive applicability of this method. Additionally, solvent use can introduce impurities, adversely affecting the purity and performance of the final product. Temperature and pressure control in liquid-phase systems is more challenging than in solid or gas-phase systems, especially when precise adjustments are necessary to optimize material properties. Alternatively, non-liquid-phase microwave-assisted synthesis, an advanced form of technology, demonstrates its progress and superiority<sup>[21,22]</sup>. This non-liquid approach, commencing with dry initial materials, eliminates the drying step post-synthesis, which is crucial for materials sensitive to structural or property alterations during drying<sup>[23-25]</sup>. It also allows finer control over reaction conditions such as temperature, pressure, and duration, essential for fine-tuning the microstructure of energy storage electrode materials<sup>[26-28]</sup>. Furthermore, by avoiding organic solvents typically used in liquid-phase reactions, non-liquid-phase synthesis is more environmentally friendly, reducing dependence on and emissions of harmful solvents<sup>[29]</sup>. Hence, advanced microwave technology, characterized by its local selective response, high controllability, rapid heating, high entropy change, and strong penetration capability, shows considerable superiority in advancing high-performance electrode materials for energy storage.

Advanced microwave synthesis techniques are increasingly prevalent in fabricating energy storage electrode materials featuring distinctive microstructures. Within the realm of microwave-assisted synthesis for energy materials, researchers have adeptly engineered a diverse array of nanomaterials, characterized by unique microstructures and superior electrochemical properties<sup>[30]</sup>. The achievement of these microstructures is facilitated by employing a spectrum of sophisticated strategies, encompassing nanosize modulation<sup>[31]</sup>, dimensional evolution<sup>[32]</sup>, composite design<sup>[33]</sup>, and defect engineering<sup>[34]</sup>, alongside consideration of crystal structure<sup>[35]</sup>. This success is attributed to the meticulous adjustment of synthesis parameters, including

microwave irradiation duration, power settings, and modifications to the inert atmosphere of the reaction system<sup>[36]</sup>. The scope of materials encompasses a spectrum of dimensionalities - ranging from zero-dimensional (0D)<sup>[37]</sup> to one-dimensional (1D)<sup>[38]</sup>, two-dimensional (2D)<sup>[39]</sup>, three-dimensional (3D)<sup>[40]</sup>, and multilevel composite structures<sup>[41]</sup>. These materials undergo specific surface and structural modifications to enhance their electrochemical performance. The repertoire includes graphene and its derivatives<sup>[42]</sup>, various carbon-based materials<sup>[43]</sup>, an array of metal oxides and sulfides<sup>[44]</sup>, metal-organic frameworks (MOFs)<sup>[45]</sup>, poly anions, and their derivatives<sup>[46]</sup>, alongside composite materials<sup>[47]</sup>. In electrochemical energy storage devices such as batteries and supercapacitors, these nanostructured materials play a pivotal role. They offer a profusion of active sites, facilitating efficient ion and electron transfer. Furthermore, they effectively mitigate the challenge of volume expansion in active materials during electrochemical charge-discharge cycles, thereby enhancing the stability and lifespan of the devices<sup>[48]</sup>. Collectively, the adoption of advanced microwave-assisted synthesis technology in crafting these specially structured materials has markedly augmented their electrochemical properties in energy storage applications. This advancement establishes a robust material foundation for enhancing battery and supercapacitor performance.

This review investigates advanced microwave-assisted synthesis techniques for generating microstructures in high-performance energy storage electrode materials and their applications in energy storage and conversion systems. The overview of the topics is illustrated in [Figure 1](#). The paper initiates by elucidating the fundamental working principles of advanced microwave-assisted synthesis, emphasizing its advantages over conventional thermal processing methods. Subsequently, it explores the impacts of microwave treatment on the microstructure of energy storage electrode materials, encompassing aspects of material preparation and surface modification. Furthermore, it extensively examines the diverse applications of these materials in energy storage systems, including batteries and supercapacitors. This provides an exhaustive overview of the electrochemical properties of materials synthesized with microwave assistance. The concluding section identifies the primary challenges facing advanced microwave technology in synthesizing energy storage materials and anticipates future research directions. This review aspires to propel the progress of advanced microwave-assisted synthesis in the realm of high-performance energy storage electrode materials.

## MICROWAVE-INDUCED MICROSTRUCTURAL ENGINEERING FOR ENERGY STORAGE MATERIALS

In this section, we delve into the pivotal role microwave-assisted synthesis plays in the microstructural engineering of materials for energy storage. Commencing with exploring the interaction principles between microwaves and matter, we specifically focus on key mechanisms, including dielectric, conductive, and magnetic losses. The dielectric properties of materials and their influence on the selectivity of microwave heating are further underscored. Following this, we elucidate how microwave technology enables precise tuning of the microstructure of materials. This encompasses considerations such as crystal growth rate, directionality, grain size, and overall morphology. Notably, we emphasize the efficacy of microwave processing in facilitating the formation of specific crystal phases and enhancing the electrical conductivity and ion diffusion properties of the materials. Concluding this discussion, we turn our attention to the beneficial effects of these microstructure modifications on the electrochemical properties of the materials. These effects encompass enhancements in specific capacitance, optimization of the voltage window, and improved cycling stability. In doing so, we underscore the significant potential of microwave technology in advancing the performance of energy storage electrode materials.

### Principles of microwave-matter interaction in material synthesis

Microwaves, a subset of non-ionizing electromagnetic radiation (EMR) with frequencies ranging from

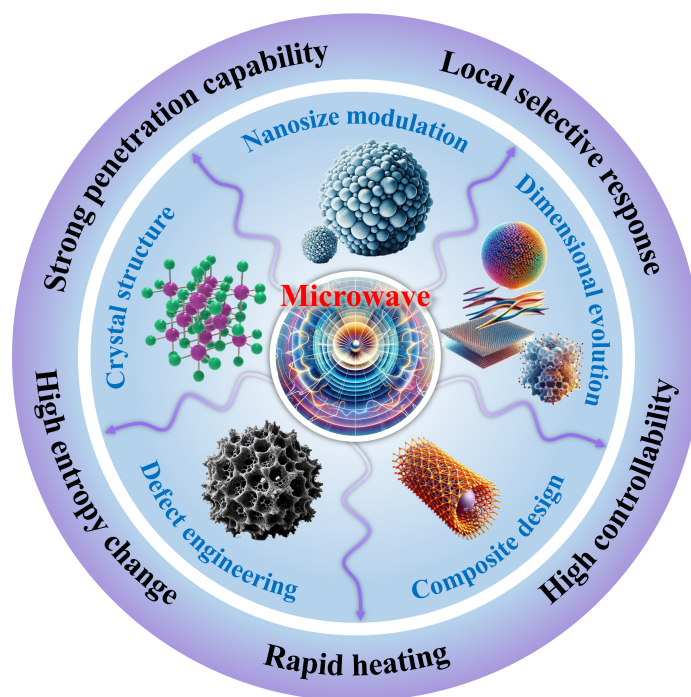


**Figure 1.** The overview of microwave for tailoring the microstructure of energy storage materials.

300 MHz to 300 GHz, assume a crucial role in material processing owing to their unique electromagnetic wave behavior. Microwave ovens, which commonly operate at a frequency of 2.45 GHz, emit microwave photons with an energy level approximately equal to  $1.0 \times 10^{-5}$  eV<sup>[49]</sup>. Although this energy is insufficient to induce alterations in molecular structure or break chemical bonds, it does influence the rotational motion of molecules. This influence gives rise to friction and collisions, ultimately transforming into thermal energy and thereby facilitating efficient heating<sup>[50]</sup>.

The mechanisms of microwave heating can be primarily categorized into three types: dielectric, conductive, and magnetic losses<sup>[51]</sup>, as shown in Figure 2A. The dielectric loss mechanism is particularly effective when processing materials containing polar molecules, such as water, ceramics, and certain organic materials. Under microwave irradiation, polar molecules in these materials, such as water molecules, attempt to align with the rapidly oscillating electric field. This alignment induces friction and vibration at the molecular level, generating heat<sup>[52]</sup>. The conductive loss mechanism is predominantly observed in materials with high electrical conductivity, such as metals, metal-based composite materials, and semiconductors. In these materials, microwave radiation induces the movement of free electrons along the direction of the electric field, generating an electric current which then converts into thermal energy<sup>[53]</sup>. The magnetic loss mechanism plays a major role in magnetic materials, involving rearranging magnetic domains and changes in the electron spin states, such as hysteresis and eddy current losses. Microwave radiation causes the reorientation and redistribution of magnetic domains in magnetic materials and adjustments in electron spin states, effectively converting magnetic energy into thermal energy<sup>[54]</sup>. Overall, these three microwave heating mechanisms each target different material characteristics, collectively forming the foundation of microwave processing technology.

Selective heating is a key characteristic of microwave processing techniques. The selectivity in heating materials with microwaves largely depends on their dielectric properties, which determine how effectively a



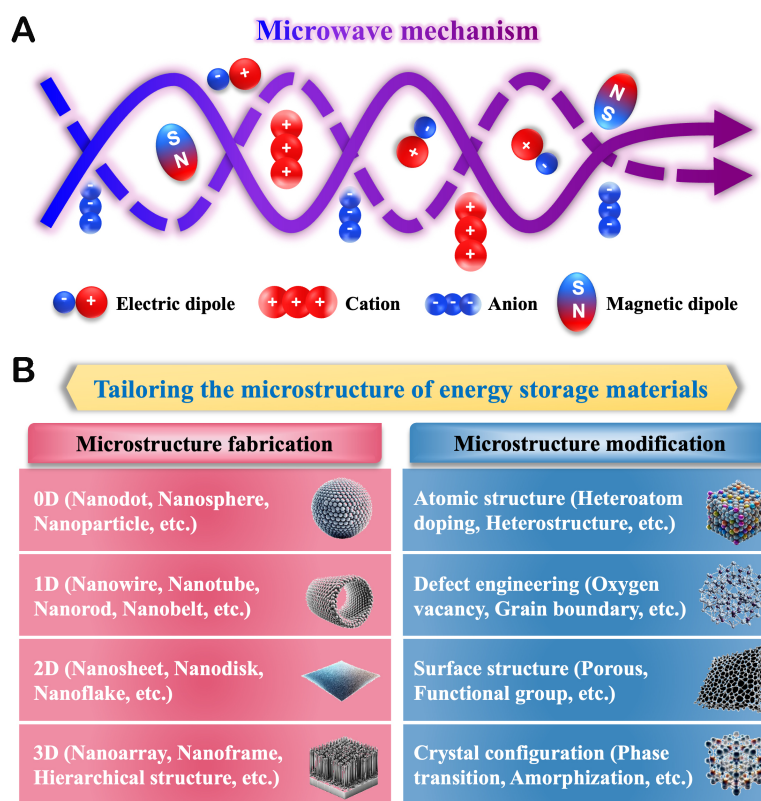


**Figure 2.** (A) The mechanism of microwave heating; (B) Tailoring the microstructure of energy storage materials.

material absorbs and dissipates microwave energy<sup>[51]</sup>. These properties are typically quantified by the dielectric loss tangent, the ratio of the dielectric constant to the dielectric loss factor. This ratio is crucial in evaluating whether a material is suitable for microwave-assisted synthesis<sup>[55]</sup>. The dielectric constant indicates how well a material can reflect and absorb incoming energy, whereas the dielectric loss factor is associated with the material's ability to convert energy dissipation, primarily from dipole polarization, into thermal energy<sup>[56]</sup>. Materials can be classified based on their microwave absorption capacity as low ( $\tan \delta < 0.1$ ), medium ( $0.1 < \tan \delta < 0.5$ ), or high absorbers ( $\tan \delta > 0.5$ ), with a higher loss tangent indicating a stronger absorption of EMR<sup>[57]</sup>. For instance, at a frequency of 2.45 GHz and room temperature, polytetrafluoroethylene (PTFE) exhibits a dielectric constant ( $\epsilon'$ ) of 2.08 and a dielectric loss factor ( $\epsilon''$ ) of 0.0008, resulting in a  $\tan \delta$  of 0.0004. This denotes a relatively weak absorption capacity of PTFE for microwave heating. In contrast, under identical conditions, water demonstrates a markedly different behavior with an  $\epsilon'$  of 80.4 and an  $\epsilon''$  of 9.89, yielding a  $\tan \delta$  of 0.123, which confers it with a moderate absorption ability in certain microwave heating applications. Moreover, carbon nanotubes (CNTs), characterized by an  $\epsilon'$  of 18 and an  $\epsilon''$  of 30, lead to a substantially higher  $\tan \delta$  of 1.67. This high dielectric loss value positions them as an ideal candidate for microwave heating processes. Notably, the lower the  $\tan \delta$  value, the higher the required microwave power for effective heating. Additionally, materials commonly used in reaction vessels, such as quartz, borosilicate, and Teflon, exhibit ultra-low  $\tan \delta$  values (close to 0), rendering them nearly transparent to microwaves. In certain instances, strong microwave absorbers, such as metal pieces, carbon nanomaterials, conducting polymers, and silicon carbide boards, can function as heat susceptors or reaction triggers when coated on vessels or substrates<sup>[58]</sup>. Thus, thoroughly analyzing the dielectric properties of a material is a crucial preliminary step in selecting appropriate materials for microwave synthesis approaches.

## Control over two-dimensional and three-dimensional structures

### *Control over two-dimensional structures*

In synthesizing 2D materials such as nanosheets or thin films, microwave technology facilitates rapid and uniform heating, which is critical for achieving consistent material properties throughout the entire structure. For example, microwave-induced dielectric heating can control the crystal growth rate and directionality, influencing the overall morphology of 2D materials. The ability to finely adjust microwave power and duration enables precise control over the thickness, grain size, and surface characteristics, endowing 2D structures with specific surface areas, porosity, and electrochemical properties<sup>[59-61]</sup>.

### *Manipulating three-dimensional structures*

In forming 3D structures such as nanoarrays or hierarchical structures, microwave technology offers significant advantages in controlling the growth and assembly of nanostructures. By selecting appropriate microwave-absorbing mediums, such as CNTs, the local temperature of the material can be rapidly increased. This, in turn, affects the uneven distribution of internal energy within the material, which may lead to localized thermal stress. This effect can facilitate the formation of complex 3D structures, which is particularly advantageous for creating materials with high porosity and specific surface structures, crucial for applications such as energy storage. By adjusting microwave parameters, the size, shape, and connectivity of these 3D structures can be tailored, customizing their functional properties<sup>[41,62]</sup>.

## Impact of microwave mechanisms on microstructural engineering

Microwave-assisted synthesis is a highly efficient material processing technology, exhibiting outstanding capabilities in controlling and improving the microstructure of energy storage materials, as shown in [Figure 2B](#). By precisely adjusting the type of microwave-absorbing medium, the level of microwave power, the duration of microwave irradiation, and the content of the precursor components, effective control over the target material can be achieved in the following aspects: Nanosize modulation, Crystal structure, Defect engineering, Composite design, and Dimensional evolution. Nanosize modulation refers to: Adjusting to produce nanomaterials with uniform size distribution and high purity through microwave assistance. For example, in microwave-assisted synthesis, non-thermal effects of microwave heating can directly transfer energy to the volume of the material, enabling rapid and uniform heating through the interaction of molecules with the electromagnetic field. Researchers optimized the synthesis of pure  $\alpha$ -phase nickel hydroxide nanosheets using microwave heating, completing the process in just ten minutes at 150 °C without surfactants or additives, effectively controlling the phase and morphology of nickel hydroxide<sup>[63]</sup>. The pure  $\alpha$ -phase nickel hydroxide nanosheets demonstrated excellent electrochemical performance in lithium-ion battery applications through microwave-assisted synthesis. Crystal structure refers to: Utilizing the thermal and non-thermal effects of microwave radiation to accelerate chemical reactions, thereby promoting the improvement of synthesized crystal quality. For instance, Fathy *et al.* prepared nanocrystalline titanium dioxide (TiO<sub>2</sub>) and reduced graphene oxide (rGO) using microwave-assisted synthesis<sup>[64]</sup>. This showed how high-quality nanomaterials could be synthesized in a short time through microwave assistance while also improving the material's photovoltaic performance. This study not only confirmed the advantages of microwave synthesis in shortening synthesis time and improving crystal quality but also demonstrated its potential in preparing low-cost, environmentally friendly solar cell materials<sup>[64]</sup>. By adjusting the parameters of microwave radiation, the crystal structure and optical properties of the material can be effectively controlled, further proving the diversity and flexibility of microwave-assisted synthesis in crystal construction. Defect engineering refers to: In the microwave-assisted synthesis process, using the characteristic of microwave EMR to act directly inside the material. By choosing suitable microwave-absorbing media (such as CNTs), the material's local temperature can be rapidly increased. This uneven energy distribution inside the material may lead to local thermal stress, thereby inducing the formation of defects, such as point (e.g., atomic vacancies and doping elements) and line defects (e.g.,

dislocations). For example, Rao *et al.* prepared  $\delta$ -MnO<sub>2</sub> petal-like nanostructures on nickel foam through microwave-assisted synthesis<sup>[65]</sup>. These 3D and oxygen-deficient nanostructures showed excellent performance with high discharge capacity and enhanced stability over 100 cycles<sup>[65]</sup>. Precise control of microwave parameters and synthesis environment can achieve fine-tuning of defects, thus customizing specific physical, chemical, and electronic properties of the material. Composite design refers to: Synthesizing nanocomposite materials with various structures through microwave assistance. For example, researchers synthesized MoS<sub>2</sub>@cellulose composite materials using microwave-assisted technology and applied them as electrode materials for supercapacitors. The MoS<sub>2</sub>@cellulose composites not only exhibited high specific capacitance, high energy, and high power density but also had excellent cycle stability<sup>[66]</sup>. Microwave-assisted synthesis can improve synthesis efficiency and material performance and provide new material options for energy storage device development. Dimensional evolution refers to: The impact of thermal effects during the microwave heating process on material characteristics, which may induce phase transitions in materials. This process can cause the dimensional size of materials to evolve from 0D, 1D to multilevel structures. Under high-temperature conditions, the energy of microwave radiation can significantly affect the internal surface diffusion and aggregation behavior of materials, thereby determining the formation of specific size structures, the generation of nanoparticles, and their properties and exhibiting excellent electrochemical performance. During the microwave-assisted synthesis process, multidimensional nanostructures, such as 0D (Nanodot, Nanosphere, Nanoparticle)<sup>[67,68]</sup>, 1D (Nanowire, Nanotube, Nanorod, Nanobelt)<sup>[69,70]</sup>, 2D (Nanosheet, Nanodisk, Nanoflake)<sup>[59]</sup>, and 3D (Nanoarray, Nanoframe, Hierarchical structure)<sup>[71-73]</sup>, can be produced by controlling factors such as microwave power, exposure time, reaction medium, and precursor concentration. Table 1<sup>[33,45,62,74-97]</sup> summarizes the energy storage electrode materials prepared/modified under various microwave parameters and reaction conditions. The distinct microstructural forms of these materials significantly influence factors such as their electrochemical performance, electrode-electrolyte interface, and the pathways for electron and ion transport. Furthermore, microwave treatment also demonstrates its formidable capability in the microstructure modification of energy storage materials. This includes adjusting the atomic structure through heteroatom doping or forming heterostructures, thereby altering the local chemical environment of the materials, which enhances their electronic structure and reaction activity<sup>[98]</sup>. Defect engineering, such as introducing oxygen vacancies and grain boundaries, is facilitated by microwave irradiation, which can create ordered or disordered defects within the materials<sup>[34]</sup>. These defects significantly improve the electrochemical properties of the materials. In terms of optimizing the surface structure, microwave treatment enhances the material's surface reactivity and ion exchange capability by introducing porous structures and functional groups<sup>[99-101]</sup>. Furthermore, microwave synthesis can induce phase transitions or promote the formation of amorphous materials, fundamentally changing the materials' electrochemical performance<sup>[22]</sup>. Through these methods, microwave-assisted synthesis not only prepares new microstructures but also effectively modifies existing materials, enhancing their performance in energy storage applications. In summary, this technique holds tremendous potential in controlling the microstructure of energy storage materials. By meticulously manipulating microwave parameters and reaction conditions, structural adjustments from the nano to the macro scale can be achieved, laying a significant technological foundation for developing new energy storage materials with superior electrochemical properties.

### Microwave-induced microstructural effects on energy storage properties

The microwave-assisted synthesis technique provides a high degree of precision in microstructural control, substantially boosting the performance of electrode materials for energy storage. Using it, researchers have successfully synthesized a range of electrode materials with superior electrochemical characteristics. These include graphene and its derivatives<sup>[102]</sup>, various carbon-based materials<sup>[103]</sup>, metal oxides<sup>[104]</sup>, metal sulfides<sup>[105]</sup>, MOFs<sup>[45]</sup>, polyanions and their derivatives<sup>[106]</sup>, and assorted composite materials<sup>[47]</sup>. Energy storage electrode materials fabricated through microwave-assisted synthesis demonstrate significant

**Table 1. Summarizes the energy storage electrode materials prepared under various microwave parameters and reaction conditions**

Applications	Materials	Preparation/modified	Structure	Heating power [W]	Heating temperature [°C]	Heating duration
LIB <sup>[74]</sup>	TiNb <sub>2</sub> O <sub>7</sub>	Preparation	Microsphere	-	200	30 min
LIB <sup>[75]</sup>	SnO <sub>2</sub>	Preparation	Nanoparticle	900	150	90 min
LIB <sup>[76]</sup>	CuS	Preparation	Nanosphere	650	-	20 min
LIB <sup>[77]</sup>	LiFePO <sub>4</sub>	Preparation	Olivine structure	40 to 50	200	60 min
LIB <sup>[78]</sup>	MoO <sub>3</sub>	Preparation	Nanobelt	500	180	10 min
LIB <sup>[79]</sup>	MoS <sub>2</sub> /Cu	Preparation	Nanowire	-	180	30 min
LIB <sup>[33]</sup>	CNTs@Ti <sub>3</sub> C <sub>2</sub>	Preparation	Hierarchical structure	900	-	40 s
SIB <sup>[62]</sup>	Sb <sub>2</sub> O <sub>3</sub> /Sb@graphene	Preparation	Hierarchical structure	750	400-800	2 min
LIB <sup>[80]</sup>	Co-Ni-BTC	Modified	Heteroatom doping	-	150	30 min
LIB <sup>[81]</sup>	N-UNCD	Modified	Heteroatom doping	-	600	6 h
PIB <sup>[82]</sup>	Co-MOF-CNT	Preparation	Nanosheet	-	130	1 h
SIB <sup>[83]</sup>	Na <sub>3</sub> V <sub>2</sub> (PO <sub>4</sub> ) <sub>3</sub>	Preparation	Hierarchical structure	800	180	1 h
SIB <sup>[84]</sup>	C	Preparation	Defect-rich porous nanosheets	300	-	5 min
SIB <sup>[85]</sup>	Sb <sub>2</sub> MoO <sub>6</sub>	Preparation	Microsphere	-	160	90 min
SIB <sup>[86]</sup>	Na <sub>3</sub> V <sub>2</sub> (PO <sub>4</sub> ) <sub>2</sub> O <sub>2</sub> F@C	Preparation	Hierarchical mulberry-shaped	-	220	10 min
SIB <sup>[87]</sup>	NaFeF <sub>3</sub> perovskite	Preparation	Nanoparticle	-	150	5 min
ZIB <sup>[88]</sup>	Na <sub>3</sub> V <sub>2</sub> (PO <sub>4</sub> ) <sub>2</sub> F <sub>3</sub>	Preparation	Nanocuboids	-	130	1 h
ZIB <sup>[89]</sup>	MnO <sub>2</sub>	Modified	Heteroatom doping	-	120	15 min
ZIB <sup>[90]</sup>	NH <sub>4</sub> V <sub>4</sub> O <sub>10</sub>	Preparation	Layered	-	200	~0.5 h
ZIB <sup>[91]</sup>	VO <sub>2</sub> ·0.2H <sub>2</sub> O	Preparation	Nanocuboid	-	200	30 min
ZIB <sup>[92]</sup>	(NH <sub>4</sub> ) <sub>2</sub> V <sub>6</sub> O <sub>16</sub> ·1.5H <sub>2</sub> O	Preparation	Nanowire	-	190	2.5 h
ZIB <sup>[93]</sup>	Zn <sub>3</sub> V <sub>2</sub> O <sub>7</sub> (OH) <sub>2</sub> ·2H <sub>2</sub> O	Preparation	Nanowire	-	180	6 h
SC <sup>[94]</sup>	Li <sub>4</sub> Ti <sub>5</sub> O <sub>12</sub>	Preparation	Nanocluster	-	160	30 min
SC <sup>[45]</sup>	C	Modified	Heteroatom doping	100	-	4 min 30 s
SC <sup>[95]</sup>	MOFs	Modified	Heteroatom doping	900	649.2	10 s
SC <sup>[96]</sup>	CNT-Mn <sub>3</sub> O <sub>4</sub> /CoWO <sub>4</sub>	Preparation	Hierarchical structure	800	160	1 h
SC <sup>[97]</sup>	CoCo <sub>2</sub> O <sub>4</sub>	Modified	Heteroatom doping	800	140	1 h

electrochemical advantages. Typically, these materials exhibit enhanced specific capacitance, a benefit attributed to the microwave treatment's ability to increase the material's specific surface area and porosity, thereby offering an abundance of active sites. Features such as optimized voltage windows and heightened cycle stability are also hallmarks of these microwave-synthesized materials<sup>[107]</sup>. This improved performance results from the microwave synthesis's

enhancement of the materials' crystallinity and conductivity, which mitigates the structural degradation of electrode materials during extended charge-discharge cycles<sup>[108]</sup>. These microwave-assisted synthesized materials have found extensive application in various electrochemical energy storage systems, including lithium-ion batteries<sup>[80]</sup>, sodium-ion batteries<sup>[46]</sup>, zinc-ion batteries<sup>[93]</sup>, and supercapacitors<sup>[109]</sup>. The high-performance attributes of these materials are effectively demonstrated in these applications. Table 2<sup>[33,45,62,74,75,77-81,83-86,88-97,110]</sup> meticulously details the energy storage electrode materials developed using microwave technology and key electrochemical performance parameters such as specific capacitance and cycle stability. This information not only validates the efficiency of microwave-assisted synthesis in fabricating energy storage electrode materials but also unveils the immense potential of this technology in elevating the performance of electrode materials. In conclusion, these research achievements contribute significantly to the advancement of energy storage technologies and underscore the critical role of advanced microwave technology in synthesizing nanoscale electrode materials.

## APPLICATIONS OF ENERGY STORAGE MATERIALS PREPARED VIA MICROWAVE

In this section, we delve into applying energy storage materials prepared through microwave-assisted synthesis methods in various energy storage devices, including lithium-ion batteries, sodium-ion batteries, zinc-ion batteries, and supercapacitors. Additionally, we thoroughly analyze the significant advantages of advanced non-liquid-phase microwave-assisted synthesis over conventional liquid-phase microwave-assisted synthesis methods. In exploring the applications in these energy storage devices, our approach is centered on the materials synthesized via microwave technology, particularly focusing on their structural and functional modification characteristics. These materials exhibit diverse structures, including 0D, 1D, 2D, 3D, and multilevel composite structures. Moreover, the scope of modification encompasses the creation of porous structures, introduction of oxygen vacancies, and heteroatom doping, all aimed at enhancing the electrochemical performance of the materials.

### Lithium-ion battery

Lithium-ion batteries, acclaimed for their exceptional energy density, enduring stability, and eco-friendly characteristics, are extensively employed across various domains<sup>[111]</sup>. Their fundamental components encompass the cathode, anode, and electrolyte. The energy storage mechanism in these batteries primarily hinges on the intercalation and deintercalation of lithium ions between the anode and cathode, particularly during discharge, where lithium ions migrate from the anode to the cathode<sup>[112,113]</sup>. As a result, the strategic development of electrode materials, distinguished by their carefully controlled nanostructured microarchitectures synthesized through microwave-assisted methods, plays a critical role in enhancing the electrochemical performance of lithium-ion batteries<sup>[114]</sup>. These nanoscale microstructures play a crucial role in significantly boosting the reactivity and ion transport efficiency within the electrode materials, thereby substantially elevating the overall functional performance of the battery system<sup>[115]</sup>.

The 0D nanostructures exhibit considerable promise in developing electrode materials for lithium-ion batteries owing to their distinctive quantum size effect and extensive specific surface area<sup>[116]</sup>. The application of microwave-assisted thermal influence facilitates the rapid and uniform formation of nanoparticles on conductive substrates. As shown in Figure 3A, the synthesis of CuS nanospheres on a CNT substrate is achieved through a microwave-assisted solvothermal method<sup>[76]</sup>. This process is particularly efficient due to the superior microwave energy absorption of CNTs compared to solvents, which accelerates the nucleation and growth of CuS on the CNT surface. In this process, the parameters of the microwave are crucial: the microwave time used is 20 min, with cyclic radiation consisting of 9 on and 21 s off, and the microwave power is set to 650 W. The influence of microwave irradiation extends beyond merely expediting the nucleation process; it also fosters a strong bond between CNTs and CuS nanospheres,



**Table 2. The electrochemical performance of energy storage electrode materials prepared by microwave-assisted synthesis**

Application	Material	Electrolyte	Voltage window	Specific capacity	Cycling stability
LIB <sup>[74]</sup>	TiNb <sub>2</sub> O <sub>7</sub>	1 M LiPF <sub>6</sub>	1.0-3.0 V	299 mAh g <sup>-1</sup>	95.5% after 100 cycles
LIB <sup>[75]</sup>	ATO/GO	1.15 M LiPF <sub>6</sub>	0.01-3.0 V	1,226 mAh g <sup>-1</sup>	77% after 1,000 cycles
LIB <sup>[77]</sup>	LiFePO <sub>4</sub>	1 M LiPF <sub>3</sub> (CF <sub>2</sub> CF <sub>3</sub> ) <sub>3</sub>	2.8-4.1 V	142 mAh g <sup>-1</sup>	97.6% after 500 cycles
LIB <sup>[78]</sup>	$\alpha$ -MoO <sub>3</sub> /SWCNH	1 M LiPF <sub>6</sub>	0.05-3 V	672 mAh g <sup>-1</sup>	over 99% after 3,000 cycles
LIB <sup>[79]</sup>	MoS <sub>2</sub> /Cu	1 M LiPF <sub>6</sub>	0.01-3 V	914.6 mAh g <sup>-1</sup>	570.6 mAh g <sup>-1</sup> after 250 cycles
LIB <sup>[33]</sup>	CNTs@Ti <sub>3</sub> C <sub>2</sub>	1 M LiPF <sub>6</sub>	0.01-3 V	430 mAh g <sup>-1</sup>	445 mA h g <sup>-1</sup> over 250 cycles
SIB <sup>[62]</sup>	Sb <sub>2</sub> O <sub>3</sub> /Sb@graphene	1 M NaClO <sub>4</sub>	0-2 V	523 mAh g <sup>-1</sup>	92.7% after 275 cycles
LIB <sup>[80]</sup>	Co-Ni-BTC	1 M LiPF <sub>6</sub>	0.005-3.0 V	-964 mAh g <sup>-1</sup>	1,051 mAh g <sup>-1</sup> after 300 cycles
LIB <sup>[81]</sup>	N-UNCD	1.2 M LiPF <sub>6</sub>	0.001- 1.5 V	350 mAh g <sup>-1</sup>	more than 98% after 100 cycles
SIB <sup>[83]</sup>	Na <sub>3</sub> V <sub>2</sub> (PO <sub>4</sub> ) <sub>3</sub> @C	-	0.6-2.2 V	117.2 mAh g <sup>-1</sup>	65 mAh g <sup>-1</sup> after 1,000 cycles
SIB <sup>[84]</sup>	SC-NSs	1 M NaPF <sub>6</sub>	-	103 mAh g <sup>-1</sup>	93% after 3,500 cycles
SIB <sup>[85]</sup>	Sb <sub>2</sub> MoO <sub>6</sub>	1 M NaClO <sub>4</sub>	0.8-3.4 V	637.3 mAh g <sup>-1</sup>	98.7% after 450 cycles
SIB <sup>[86]</sup>	Na <sub>3</sub> V <sub>2</sub> (PO <sub>4</sub> ) <sub>2</sub> O <sub>2</sub> F@C	1 M NaClO <sub>4</sub>	2.5-4.5 V	127.9 mAh g <sup>-1</sup>	82.1% after 2,000 cycles
ZIB <sup>[88]</sup>	Na <sub>3</sub> V <sub>2</sub> (PO <sub>4</sub> ) <sub>2</sub> F <sub>3</sub> @rGO	2.5 M C <sub>2</sub> F <sub>6</sub> O <sub>6</sub> S <sub>2</sub> Zn	0.4-1.9 V	126.9 mAh g <sup>-1</sup>	90.6% after 60 cycles
ZIB <sup>[89]</sup>	d-MnO <sub>2</sub>	2 M ZnSO <sub>4</sub> + 0.2 M MnSO <sub>4</sub>	1.0-1.8 V	455 mAh g <sup>-1</sup>	80% after 500 cycles
ZIB <sup>[90]</sup>	NH <sub>4</sub> V <sub>4</sub> O <sub>10</sub>	3 M Zn(CF <sub>3</sub> SO <sub>3</sub> ) <sub>2</sub>	1.2-0.2 V	417 mAh g <sup>-1</sup>	75% after 150 cycles
ZIB <sup>[91]</sup>	Zn/VOG	2 M ZnSO <sub>4</sub>	0.4-1.1 V	423 mAh g <sup>-1</sup>	84.7% after 1,000 cycles
ZIB <sup>[110]</sup>	MnO <sub>2</sub>	3 M ZnSO <sub>4</sub> + 0.2 M MnSO <sub>4</sub>	1.0-1.8 V	288 mAh g <sup>-1</sup>	91.8% after 200 cycles
ZIB <sup>[92]</sup>	(NH <sub>4</sub> ) <sub>2</sub> V <sub>6</sub> O <sub>16</sub> ·1.5H <sub>2</sub> O	3 M Zn(CF <sub>3</sub> SO <sub>3</sub> ) <sub>2</sub>	0.4-1.6 V	423 mAh g <sup>-1</sup>	75% after 10,000 cycles
ZIB <sup>[93]</sup>	Zn <sub>3</sub> V <sub>2</sub> O <sub>7</sub> (OH) <sub>2</sub> ·2H <sub>2</sub> O	1 M ZnSO <sub>4</sub>	0.2-1.8 V	213 mAh g <sup>-1</sup>	68% after 300 cycles
SC <sup>[94]</sup>	Li <sub>4</sub> Ti <sub>5</sub> O <sub>12</sub>	1 M LiPF <sub>6</sub>	1.0-3.0 V	97.2 mAh g <sup>-1</sup>	2,000 cycles with an ultralow decay rate of 0.003% per cycle
SC <sup>[45]</sup>	CD-MOF	1 M H <sub>2</sub> SO <sub>4</sub>	-	501 F g <sup>-1</sup>	90.1% after 5,000 cycles
SC <sup>[95]</sup>	Zn,Ni-CAT	3 M KCl	0-0.5 V	422.54 mF cm <sup>-2</sup>	91.53% after 30,000 cycles
SC <sup>[96]</sup>	CNT-Mn <sub>3</sub> O <sub>4</sub> /CoWO <sub>4</sub>	6 M KOH	1.15 V	529.8 mA h g <sup>-1</sup>	117.2% after 13,000 cycles
SC <sup>[97]</sup>	Mn <sub>2</sub> CoCo <sub>2</sub> O <sub>4</sub>	6 M KOH	1.1 V	424.4 mA h g <sup>-1</sup>	83.7 % for 8,000cycles

thereby constructing a 3D electron conduction network. This network plays a critical role in optimizing electron mobility and reaction kinetics, offering structural stability against volume expansion during charge and discharge cycles in lithium-ion batteries and significantly improving the reversible and rate performance of the electrode material. Notably, after 450 cycles, the CuS/0.5CNT material demonstrated a capacity of 569 mAh g<sup>-1</sup> at a current density of 400 mA g<sup>-1</sup>. Impressively, even at a high current density of 6,400 mA g<sup>-1</sup>, the CuS/0.5CNT material sustained a reversible capacity of approximately 400 mAh g<sup>-1</sup>. Furthermore, the application of microwave technology has been extended to the synthesis of metal oxide microspheres. [Figure 3B](#) illustrates the work of

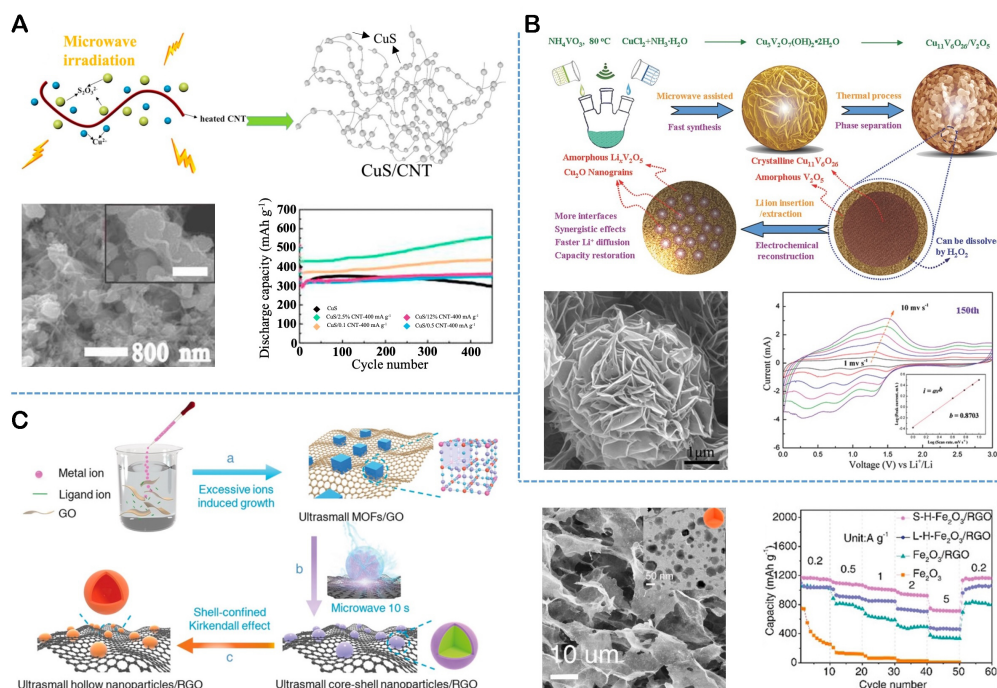


**Figure 3.** (A) CuS nanospheres fabricated on CNTs via the liquid-phase microwave method, and their cyclic stability in lithium-ion battery applications. This figure is quoted with permission<sup>[76]</sup>; (B) Cu<sub>11</sub>V<sub>6</sub>O<sub>26</sub>/V<sub>2</sub>O<sub>5</sub> microspheres with a core/shell structure prepared using a liquid-phase microwave method and their capacity self-recovery characteristics in lithium-ion battery applications. This figure is quoted with permission<sup>[117]</sup>; (C) Oxide nanoparticles grown on the rGO surface using a gas-phase microwave method and their energy storage performance in lithium-ion batteries. This figure is quoted with permission<sup>[118]</sup>.

Pei *et al.*, who synthesized the Cu<sub>3</sub>V<sub>2</sub>O<sub>7</sub>(OH)<sub>2</sub>·2H<sub>2</sub>O precursor using a microwave-assisted solvothermal method<sup>[117]</sup>, applying microwave heating for 8 min at 100 °C. This process resulted in the formation of 2D nanosheets, ranging from 20 to 30 nm in thickness, which self-assembled into flower-like structures. Subsequent annealing treatment led to the creation of Cu<sub>11</sub>V<sub>6</sub>O<sub>26</sub>/V<sub>2</sub>O<sub>5</sub> microspheres characterized by a 3D layered structure. In the context of lithium-ion batteries, this material demonstrated a remarkable reversible capacity of up to 1,110 mAh g<sup>-1</sup> and a significant capacity for self-recovery. In a similar vein, Gupta *et al.* successfully fabricated TiNb<sub>2</sub>O<sub>7</sub> microspheres employing the microwave-assisted solvothermal method<sup>[74]</sup>. This distinct microsphere structure boasted a superior lithium-ion diffusion coefficient ( $1.21 \times 10^{-13}$  cm<sup>2</sup> s<sup>-1</sup>), surpassing the performance of samples prepared through conventional methods by 1.5 times. When discharged at a rate of 0.1 C, the microwave-synthesized sample exhibited a high discharge capacity of 299 mAh g<sup>-1</sup>, compared to 278 mAh g<sup>-1</sup> for those synthesized via the solvothermal method. This underscores the significant advantages of microwave synthesis technology in enhancing the performance of electrode materials for lithium-ion batteries. Furthermore, compared to liquid-phase microwave synthesis, advanced gas-phase microwave irradiation offers greater control over the crystal nanostructure. As shown in Figure 3C, Fan *et al.* demonstrated that by applying microwave radiation to promptly increase the surface temperature of graphene oxide, MOF nanoparticles were rapidly disintegrated into metals and volatile gases<sup>[118]</sup>. This formed ultra-small hollow nanoparticles composed of multi-metal oxides, phosphides, and sulfides, exhibiting superior electrochemical characteristics. These nanoparticles are characterized by diameters smaller than 20 nm and shell thicknesses less than 3 nm. Compared to larger hollow nanostructures, these diminutive hollow structures, such as Fe<sub>2</sub>O<sub>3</sub>, demonstrate enhanced lithium-ion storage capabilities. This enhancement is attributed to their faster charge transfer, increased number of active sites, and effective management of stress due to volume changes. Evidently, they exhibit an impressive

reversible capacity of  $1,167 \text{ mAh g}^{-1}$  at  $0.2 \text{ A g}^{-1}$  and rate performance of  $701 \text{ mAh g}^{-1}$  at  $5 \text{ A g}^{-1}$  and maintain 97.8% of their cycle stability after 1,200 cycles at  $5 \text{ A g}^{-1}$ . Therefore, microwave heating can quickly and evenly heat nanoparticles, which helps obtain uniform particle sizes and good crystal structures. This is very important for improving the specific capacity and cycle stability of lithium-ion batteries.

Microwave-assisted synthesis is not solely limited to generating 0D nanostructures; it also encompasses creating 1D nanowires and 2D nanosheets, thereby introducing alternative perspectives in developing materials for energy storage electrodes<sup>[119]</sup>. Yoon *et al.* employed a microwave-assisted solvothermal method to synthesize carbon-decorated  $\text{WO}_x\text{-MoO}_2$  nanorod ( $x = 2$  and  $3$ ), significantly reducing the reaction time<sup>[120]</sup>. These nanorods, due to the elastic matrix of the carbon layer, exhibit exceptional volumetric adaptability and anti-aggregation properties during charge-discharge cycles, resulting in impressive capacitance retention. After 50 cycles, the capacitance remained stable at  $670 \text{ mA h g}^{-1}$ . In comparison to liquid-phase microwave synthesis, advanced solid-phase microwave technology eliminates the need for solvents, thereby significantly reducing environmental impact. As shown in Figure 4A, the team led by an utilized a microwave-assisted solid-state synthesis approach to create layered manganese oxide nanotubes with a distinctive hollow and porous wall structure enveloped in carbon layers<sup>[121]</sup>. The microwave process facilitated the development of porous structures on the manganese oxide nanotubes, noticeable at  $400^\circ\text{C}$ , with the pores enlarging as the microwave temperature increased. The experimental data revealed that these carbon-encapsulated hollow manganese oxide nanotubes retained a considerable reversible capacity of  $875 \text{ mA h g}^{-1}$  even after 100 cycles, along with displaying superior rate performance maintaining capacities between 700 and  $729 \text{ mA h g}^{-1}$ . In electrochemical energy storage systems, 1D materials are known for their enhanced electrical conductivity and swift ion transport due to their unique geometry. Similarly, 2D materials, recognized for their vast specific surface areas and excellent electron conductivity, are increasingly important in energy storage applications. Figure 4B illustrates the successful synthesis of  $\alpha\text{-MoO}_3$  nanohorns on single-walled CNTs (SWCNTs) by Sahu *et al.*, achieved through a microwave-assisted solvothermal method<sup>[178]</sup>. In this process, the materials were exposed to a microwave power of 500 W at  $180^\circ\text{C}$  for 10 min, facilitating the formation of the desired nanostructures. This structure is adept at providing a rapid 3D Co-diffusion channel for lithium ions, especially under conditions of high-rate charge and discharge. The point contact established between the  $\alpha\text{-MoO}_3$  nanohorns and the SWCNT tips forms an efficient network for electron and lithium-ion transport, a crucial aspect for enhancing the efficiency of the charge-discharge cycle. Experimental observations revealed that the  $\alpha\text{-MoO}_3\text{/SWCNT}$  composite manifested a high specific capacity, reaching  $654 \text{ mAh g}^{-1}$  at a 1C discharge rate. Impressively, it sustained a substantial capacity of  $275 \text{ mAh g}^{-1}$  even under a 5C rate. Most notably, after undergoing 3,000 charge-discharge cycles, the composite showcased exceptional capacity retention, maintaining 99% of its capacity at a 1 C rate, underscoring its outstanding cycle stability. Figure 4C demonstrates the transformation of 2D  $\text{LiCoO}_2$  nanosheets into cathode materials suitable for lithium-ion batteries<sup>[122]</sup>. This conversion is achieved through a microwave-assisted hydrothermal treatment, conducted at  $160^\circ\text{C}$  for 30 min, followed by a subsequent annealing process. The microwave treatment not only enhances the efficiency of the synthesis but also plays a pivotal role in developing a 2D non-equilibrium structure in the lithium cobalt oxides, which is critical for their electrochemical performance. In assessing electrochemical properties, the synthesized LCO nanosheets exhibited a high initial discharge capacity of about  $131 \text{ mAh g}^{-1}$ . Figure 4D presents the ultrathin birnessite  $\text{K}_{0.17}\text{MnO}_2$  nanosheets, synthesized using a microwave-assisted solvothermal method, intended for use in lithium-ion battery cathodes<sup>[123]</sup>. The synthesis process involves heating in a microwave at  $120^\circ\text{C}$  for 5 min, a step critical to achieving the desired structure and properties. The  $\text{K}_{0.17}\text{MnO}_2$  nanosheets, in synergy with their inherent 2D crystal structure, offer numerous advantages such as a large surface area, facile ion diffusion, and efficient electron transport. These attributes collectively underpin the exceptional cycling performance of the nanosheets, as they exhibit a capacity retention exceeding 93% even after undergoing 1,000 consecutive operational cycles. Therefore, in the microwave-assisted synthesis process, microwave

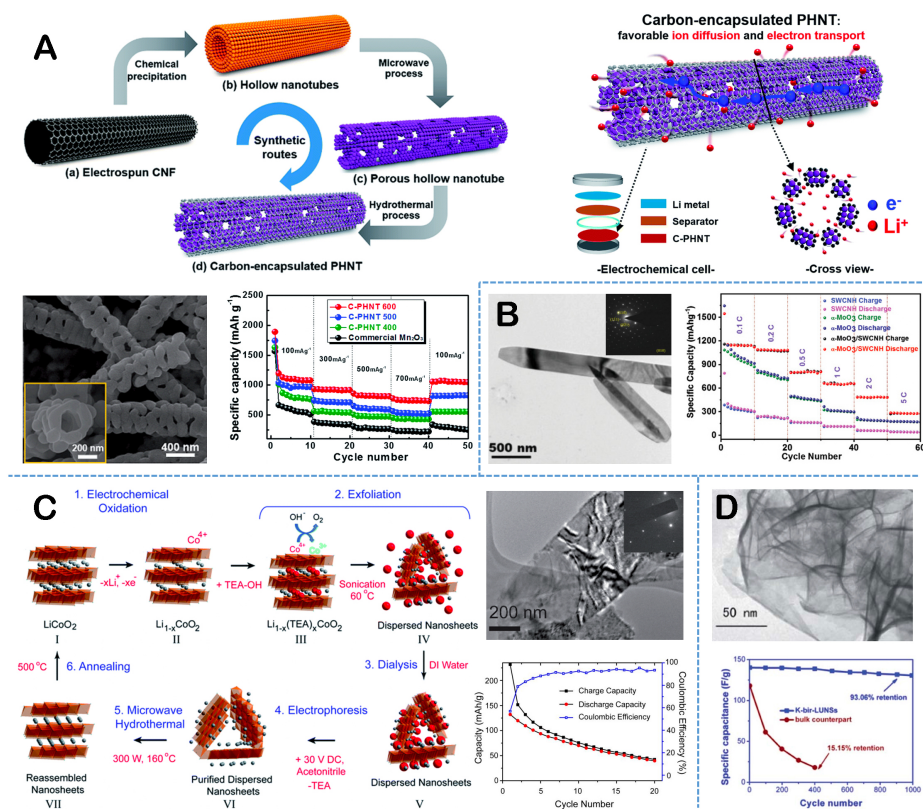


**Figure 4.** (A) Layered carbon-encapsulated manganese oxide nanotubes fabricated via the solid-phase microwave method, featuring their reversible capacity in lithium-ion battery applications. This figure is quoted with permission<sup>[121]</sup>; (B)  $\alpha$ -MoO<sub>3</sub> nanobelts prepared on SWCNTs using the liquid-phase microwave method, highlighting their specific capacity in lithium-ion battery applications. This figure is quoted with permission<sup>[78]</sup>; (C) LiCoO<sub>2</sub> nanosheets produced by the liquid-phase microwave method, showcasing their charge-discharge capacity in lithium-ion battery applications. This figure is quoted with permission<sup>[122]</sup>; (D) K<sub>0.17</sub>MnO<sub>2</sub> nanosheets prepared through the liquid-phase microwave method, demonstrating their cycle stability in lithium-ion battery applications. This figure is quoted with permission<sup>[123]</sup>.

technology can facilitate the rapid growth of 1D and 2D materials while maintaining the structural integrity of the materials.

The 3D and multilevel composite structures play a key role in enhancing the electrochemical activity of electrodes by providing a wider storage space for electrolytes due to their significantly high porosity compared to 1D and 2D structures. Their complex ion transport paths help to accelerate the migration of ions and electrons, which is particularly important for improving the efficiency of battery charging and discharging<sup>[124]</sup>. Microwave technology has demonstrated its unique advantages and application potential in preparing 3D and multilevel composite structure energy storage electrode materials. Figure 5A shows the successful synthesis of hollow  $\alpha$ -Fe<sub>2</sub>O<sub>3</sub> nanotubes/SnO<sub>2</sub> nanorods/rGO (FNT/S/rGO) ternary composites through a microwave-assisted solvothermal method<sup>[125]</sup>, conducted at a reaction temperature of 150 °C for 5 min. The microwave-assisted solvothermal method can control the directional growth and morphology of SnO<sub>2</sub> nanorods on the surface of  $\alpha$ -Fe<sub>2</sub>O<sub>3</sub> nanotubes more precisely than the traditional synthesis methods. The rapid heating and cooling phases in the synthesis process help reduce defects and irregularity in the structure, potentially improving the structural integrity and electrochemical properties of the material. The FNT/S/rGO anode provides a highly reversible capacity of 883 mAh g<sup>-1</sup> even at a current density of



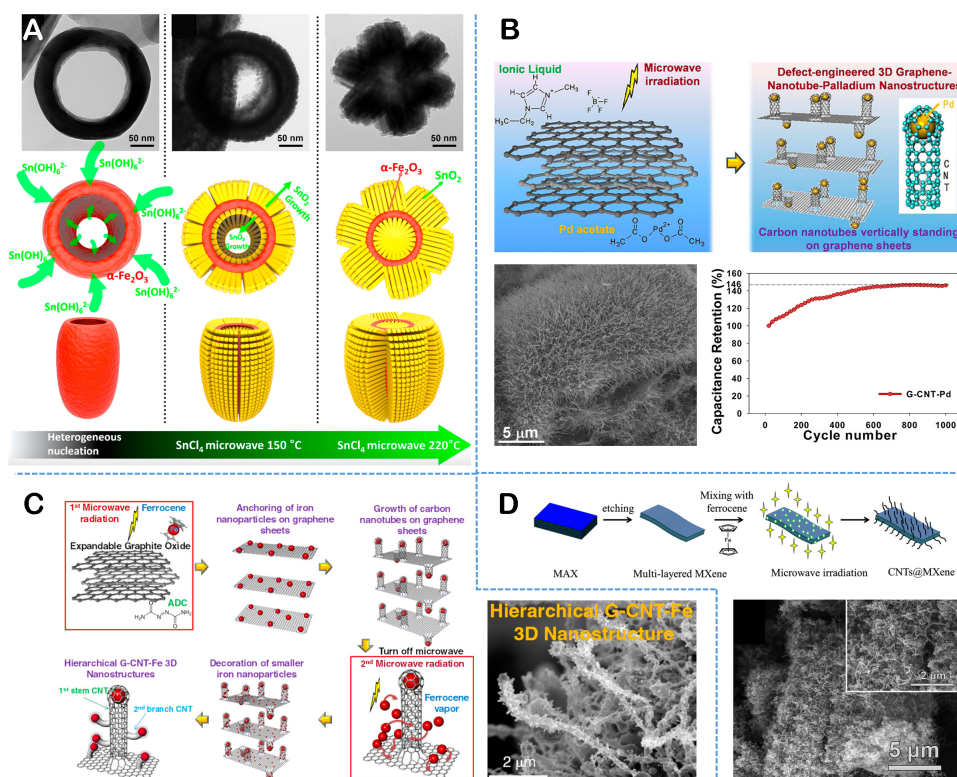


**Figure 5.** (A) 3D FNT/S/rGO composite material prepared using the liquid-phase microwave method. This figure is quoted with permission<sup>[125]</sup>; (B) 3D carbon nanostructure G-CNT-Pd prepared using the gas-phase microwave method and its characteristics of cyclic stability in lithium-ion battery applications. This figure is quoted with permission<sup>[126]</sup>; (C) 3D functional nanostructure G-CNT-Fe prepared using the gas-phase microwave method. This figure is quoted with permission<sup>[127]</sup>; (D) CNTs prepared on MXene substrates using the gas-phase microwave method. This figure is quoted with permission<sup>[33]</sup>.

200 mA g<sup>-1</sup>, with excellent high-rate capacity (382 mAh g<sup>-1</sup> at 4,320 mA g<sup>-1</sup>). In addition to the conventional liquid-phase microwave method, the advanced gas-phase microwave irradiation technology can show the advantages of faster and higher energy reaction. Figure 5B shows the synthesis of graphene-CNT-palladium (G-CNT-Pd) 3D carbon nanostructures using microwave irradiation with a power of 700 W for a reaction time of 10 min to grow CNT forests on the graphene surface<sup>[126]</sup>. Microwave radiation can induce defects on the graphene nanosheets, which act as the core and anchor points of the palladium nanoparticles. Continuous microwave irradiation causes the CNTs to grow vertically on the graphene surface, thereby forming a defect promoting mechanism that binds directly to the graphene, further strengthening the stability of the 3D nanostructures. After 600 cycles, it was observed that the capacitance increased by 46% relative to the initial capacitance, indicating that the electrode had good electrochemical stability. Similar to the 3D carbon nanostructures of G-CNT-Pd, Lee *et al.* prepared 3D functional nanostructures of G-CNT-Fe, as shown in Figure 5C<sup>[127]</sup>. During the synthesis process, microwave radiation with a power of 700 W was applied for 120 s. This radiation promoted the longitudinal growth of CNTs on the graphene matrix. And induced the formation of finer CNTs in the main duct and its branches. During this process, iron oxide nanoparticles are evenly decorated in this 3D structure, enhancing lithium-ion storage properties and increasing specific capacity. In addition, the structural transition from graphene oxide to graphene nanomites was achieved through the gas generated by the decomposition of azodicarbonamide in microwave treatment, a change that provides significantly improved performance characteristics for lithium-ion batteries. In cyclic stability evaluations, the material demonstrated a reversible capacity of



approximately  $1,024 \text{ mA}\cdot\text{h}\cdot\text{g}^{-1}$  and a coulomb efficiency of more than 99%. As shown in Figure 5D, Zheng *et al.* successfully prepared CNTs@MXene nanocomposites using microwave irradiation and carbon fiber as catalysts to induce the uniform growth of CNTs on MXene substrate at room temperature<sup>[33]</sup>. In this method, the distribution of CNTs on the MXene surface was optimized by microwave treatment lasting 40 s at a power of 900 W, the overlap and collapse of MXene layers were prevented, and a conductive network was formed between them. The thermal conductivity properties and active sites of MXene further promoted the uniform growth of CNTs. The CNTs@MXenes composite achieves high reversible capacities of 430 and  $175 \text{ mAh g}^{-1}$ , respectively, at current densities of 1 and  $10 \text{ A g}^{-1}$  ( $31.25^\circ\text{C}$ ) when used as a negative electrode material in lithium-ion batteries. Therefore, materials with 3D porous or network structures can achieve highly ordered and interconnected pore structures through microwave synthesis. Such structures facilitate the rapid diffusion of lithium ions and efficient electron transport, thereby enhancing the power density and energy density of lithium-ion batteries.

Researchers have extensively utilized microwave-assisted synthesis techniques to fabricate materials with specific structures that demonstrate enhanced properties for energy storage devices. Additionally, microwave technology is frequently employed in material modification processes<sup>[128,129]</sup>. Microwave radiation facilitates the introduction of functional groups or the creation of porous structures on material surfaces. These microstructures are instrumental in increasing the specific surface area of the electrode and optimizing the interface contact between the electrolyte and electrode material, leading to significant improvements in electrochemical performance. One primary application of microwave-assisted synthesis is in preparing porous materials. For instance, as shown in Figure 6A, Dai *et al.* adeptly synthesized Ni-Sn-P@C-CNT mesoporous hybrid microspheres utilizing a microwave-assisted solvothermal approach<sup>[130]</sup>, conducted at a microwave temperature of  $500^\circ\text{C}$  for 30 min. Integrating microwave technology not only encouraged the uniform formation of a carbon layer but also ensured the homogeneous distribution of CNTs within the microspheres, facilitated by the synergistic catalysis of Ni and Sn. As an anode material for lithium-ion batteries, the Ni-Sn-P@C-CNT material sustained a high capacity of  $704 \text{ mAh g}^{-1}$  after 200 charge and discharge cycles at a current density of  $100 \text{ mA g}^{-1}$ . As shown in Figure 6B, Wu *et al.* effectively fabricated holey 2D ultrathin oxide cathode nanosheets using a microwave-assisted solvothermal method at 700 W power<sup>[61]</sup>. The critical aspect of this technique was accelerating the formation of ultra-thin precursor nanosheets with microwave assistance. The Ni-rich oxide nanosheets exhibited high initial discharge capacities of 205.4, 198.6, 184.5, and  $168.6 \text{ mAh g}^{-1}$  at a current density of  $0.1 \text{ C}$ . Wang *et al.* have successfully synthesized a novel mesoporous, rose-like  $\text{ZnCo}_2\text{O}_4$  (ZCO) anode material for lithium-ion batteries using the microwave-assisted solvothermal technique, as shown in Figure 6C<sup>[131]</sup>. The synthesis process involved heating the material at  $195^\circ\text{C}$  for 15 min using microwave irradiation. This specific time and temperature setting is crucial for achieving the desired material properties. The particles of the (Zn,Co)-organic hybrid precursor exhibit a rose-like structure, consisting of cambered sheets with a thickness of 20-30 nm. This distinctive morphology is primarily due to the decomposition of organic components during microwave treatment, which facilitates pore formation. Serving as an anode material in lithium-ion batteries, this material demonstrates a high reversible capacity, reaching up to 1,000 milliamperes-hours per gram, under a current density of 50 milliamperes per gram. Moreover, advanced gas-phase microwave irradiation, serving as an efficient mode of energy input, plays a crucial role in the material doping process. In the study by Cheng *et al.*, as shown in Figure 6D, they skillfully developed a nitrogen-incorporated ultrananocrystalline diamond (N-UNCD) coating for the anode material of lithium-ion batteries, utilizing microwave plasma-enhanced CVD technology<sup>[81]</sup>. This process involved exposing the natural graphite (NG) electrode to microwave treatment at  $600^\circ\text{C}$  for 6 h. The principal merit of this technological advancement resides in the capacity of N-UNCD coatings to proficiently mitigate the issues associated with volumetric expansion, amorphous characteristics, and structural deformations encountered by NG electrodes during the lithium-ion intercalation and deintercalation processes. Remarkably, after 100 charge and discharge

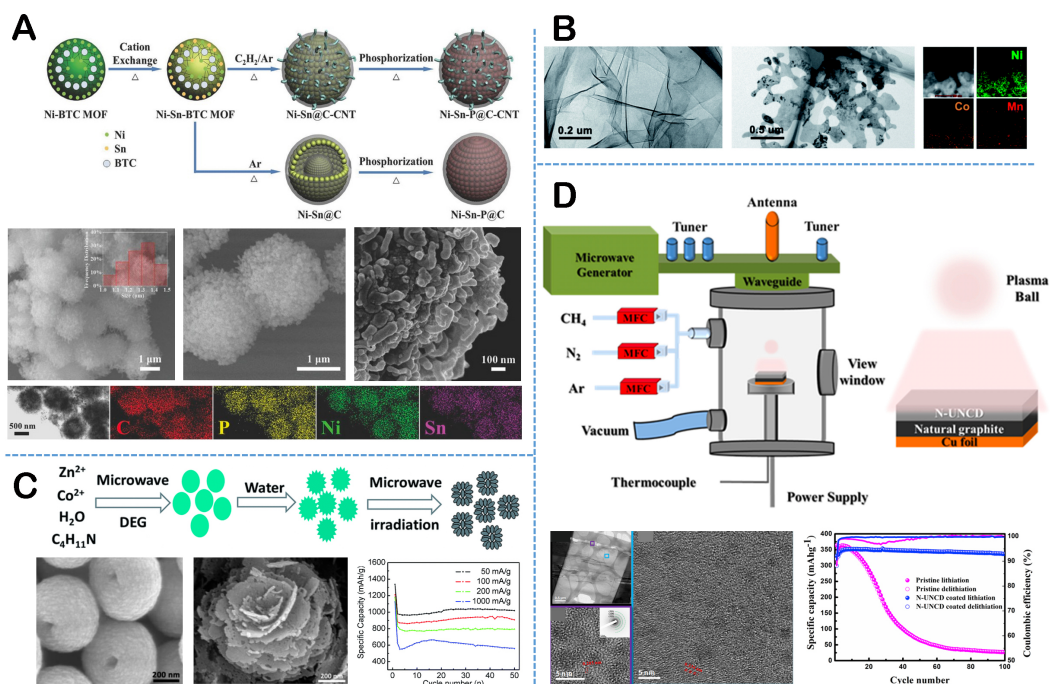


**Figure 6.** (A) Porous Ni-Sn-P@C-CNT materials prepared using the liquid-phase microwave method. This figure is quoted with permission<sup>[130]</sup>; (B) Ni-rich porous oxide nanomaterials fabricated using the liquid-phase microwave method. This figure is quoted with permission<sup>[61]</sup>; (C) Mesoporous nanostructured ZnCo<sub>2</sub>O<sub>4</sub> prepared via the liquid-phase microwave method, along with characteristics of their reversible capacity in lithium-ion battery applications. This figure is quoted with permission<sup>[131]</sup>; (D) Nitrogen-incorporated ultrananocrystalline diamond coatings, synthesized through the gas-phase microwave method, exhibit enhanced cycle stability in lithium-ion battery applications. This figure is quoted with permission<sup>[81]</sup>.

cycles, the N-UNCD-coated NG anode demonstrated a capacity retention rate of over 98%, significantly outperforming the uncoated NG anode, which showed a capacity retention rate of less than 15%. Therefore, microwave treatment can affect the crystal structure and pore structure of materials, thereby improving their electrochemical performance. For example, it can increase the specific surface area of the material and improve ion transport channels.

### Other metal-ion batteries

Confronted with the looming prospect of lithium resource scarcity and escalating energy storage costs, the widespread deployment of lithium-ion batteries in future energy storage applications encounters significant challenges<sup>[132]</sup>. In light of this, alternative metal ion batteries such as sodium-, potassium-, and zinc-ion batteries, benefiting from the relative abundance of their raw materials, are increasingly becoming the focus of research<sup>[133,134]</sup>. These alternatives are considered potential substitutes for lithium-ion batteries<sup>[135]</sup>. Researchers are actively engaged in developing electrode materials for these batteries, employing technologies such as microwave-assisted synthesis. This approach aims to enhance their electrochemical performance, prolong their service life, and reduce production costs. The microwave-assisted synthesis method can effectively control the microstructure of electrode materials, thereby optimizing the electrochemical reactivity of electrodes to meet the growing demand for energy storage.

The 0D nanostructure, owing to its unique physical and chemical properties, is extensively utilized in various metal ion batteries. **Figure 7A** illustrates the successful preparation of NaTi<sub>2</sub>(PO<sub>4</sub>)<sub>3</sub> nanoparticles, sized between 30 and 40 nm, on a rGO substrate using a microwave-assisted solvothermal method,

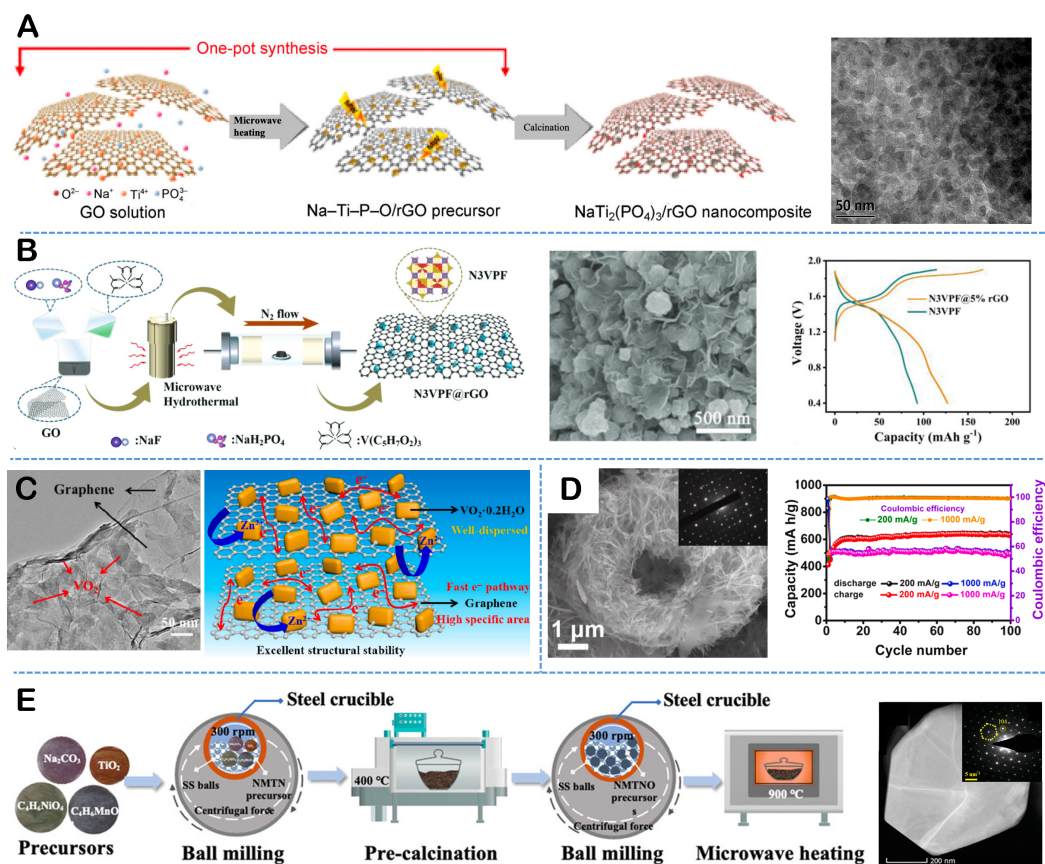


**Figure 7.** (A)  $\text{NaTi}_2(\text{PO}_4)_3$  nanoparticles prepared on rGO substrates using the liquid-phase microwave method. This figure is quoted with permission<sup>[136]</sup>; (B) Mesoporous graphene oxide-encapsulated  $\text{Na}_3\text{V}_2(\text{PO}_4)_2\text{F}_3$  ( $\text{N}_3\text{VPF}$ ) nanocuboids prepared via the liquid-phase microwave method, with a focus on their rate capability characteristics in zinc-ion battery applications. This figure is quoted with permission<sup>[88]</sup>; (C)  $\text{VO}_2 \cdot 0.2\text{H}_2\text{O}$  nanocuboids grown on graphene sheets, fabricated using the liquid-phase microwave method. This figure is quoted with permission<sup>[88]</sup>; (D)  $\text{Sb}_2\text{MoO}_6$  microspheres prepared by the liquid-phase microwave method, highlighting their reversible capacity in sodium-ion battery applications. This figure is quoted with permission<sup>[85]</sup>; (E) NMTNO nanocrystals prepared using the solid-phase microwave method. This figure is quoted with permission<sup>[137]</sup>.

achieving uniform deposition on the substrate<sup>[136]</sup>. During microwave heat treatment, the selective heating effect of microwaves on rGO significantly enhances the uniform distribution of Na-Ti-P-O precursor nanoparticles on the rGO surface. This method surpasses traditional solvothermal techniques in controlling nanoparticle growth during heat treatment and ensuring their crystalline structure integrity. When applied as an anode material in a sodium-ion battery, this nanocomposite maintained a high specific capacity of 72.9% even at a discharge rate of up to 50 C, exhibiting only a 4.5% capacity loss after 1,000 charge-discharge cycles. Figure 7B depicts the creation of regular  $\text{Na}_3\text{V}_2(\text{PO}_4)_2\text{F}_3$  ( $\text{N}_3\text{VPF}$ ) nanocuboids, ranging from 80 to 220 nm in size, covered with mesoporous graphene oxide using a microwave-assisted solvothermal method<sup>[88]</sup>. The process involves a reaction time of 1 h at a microwave temperature of 130 °C. The microwave treatment aids in forming uniform  $\text{N}_3\text{VPF}$  nanocuboids, while incorporating rGO enhances the material's electronic conductivity. As a cathode material in aqueous zinc-ion batteries, this substance demonstrates a substantial capacity of 126.9 mAh g<sup>-1</sup>, when cycled at a 0.5 C rate. Similarly, in Figure 7C, Jia *et al.* successfully synthesized  $\text{VO}_2 \cdot 0.2\text{H}_2\text{O}$  nanocuboids anchored on graphene sheets via a microwave-assisted solvothermal method<sup>[91]</sup>. In this process, the reaction temperature was meticulously controlled to reach 200 °C in 15 min and maintained for an additional 30 min. The microwave treatment not only

prevented the overlapping of graphene sheets but also mitigated the volume expansion of  $\text{VO}_2 \cdot 0.2\text{H}_2\text{O}$ . As a cathode material for aqueous zinc-ion batteries, the  $\text{VO}_2 \cdot 0.2\text{H}_2\text{O}$ /graphene composite exhibited an extremely high specific capacity of up to  $423 \text{ mAh g}^{-1}$  at a current density of  $0.25 \text{ A g}^{-1}$ . However, preparing 0D nanostructures using special carbonaceous materials often entails high costs and a complex, cumbersome synthesis process. Additionally, introducing carbonaceous materials can result in a low tap density of the electrode, which is not conducive to practical applications. Thus, developing alternative electrode materials that can achieve high performance without carbonaceous materials is crucial. In this context, Lu *et al.*, as shown in Figure 7D, synthesized mixed metal oxide microspheres containing Mo using a microwave-assisted solvothermal method, with a reaction time of 90 min and a microwave temperature of  $160^\circ\text{C}$ , aiming to address these challenges<sup>[85]</sup>. Microwave synthesis plays a pivotal role in fabricating layered  $\text{Sb}_2\text{MoO}_6$  microspheres. This unique structure contributes to forming a self-constructed conductive Na-Mo-O buffer matrix during the charge/discharge process. This matrix is not only instrumental in buffering the volume expansion associated with Na-Sb alloying/dealloying processes but also provides excellent electronic conductivity. When employed as an anode material for sodium-ion batteries, this material demonstrates a robust reversible capacity of  $637.3 \text{ mA g}^{-1}$  at a current density of 200 and  $498.7 \text{ mA g}^{-1}$  at  $1,000 \text{ mA g}^{-1}$  after 100 cycles, indicating its high electrochemical stability and performance. Compared to the microwave-assisted solvothermal method, solid-state microwave radiation synthesis technology exhibits superior synthesis efficiency and reaction uniformity. It maintains the integrity of the crystal structure while significantly reducing reaction time and energy consumption. Sengupta *et al.*, as shown in Figure 7E, successfully synthesized  $\text{P}_2$ -type  $\text{Na}_{2/3}\text{Ni}_{1/3}\text{Mn}_{7/2}\text{Ti}_{7/2}\text{O}_2$  (NMTNOnano) nanocrystalline electrode material using a microwave irradiation synthesis method<sup>[137]</sup>. This synthesis was conducted by irradiating the material in a microwave furnace at  $800^\circ\text{C}$  for 30 min. This synthesis method enhances the refinement of secondary particles and the formation of nanoscale primary crystals, thereby augmenting the overall properties of the material. Compared to micron-sized  $\text{Na}_{2/3}\text{Ni}_{1/3}\text{Mn}_{1/2}\text{Ti}_{1/2}\text{O}_2$  materials, NMTNOnano exhibited a higher specific surface area, more distinct sodium diffusion paths, and increased active sites for sodium ion intercalation and deintercalation, which improved its affinity with the electrolyte. These exceptional microstructural properties endow the NMTNOnano cathode material with a high initial discharge capacity at a  $0.1 \text{ C}$  current density and a substantial capacity retention rate after 500 cycles. The microwave-assisted synthesis method significantly enhances the preparation of energy storage electrode materials by rapidly generating nanoparticles, improving uniformity in particle size distribution, and enhancing electrochemical performance through controlled crystalline structure.

The application of 1D nanowires and 2D nanosheets, produced through microwave-assisted synthesis and the multistage structures derived from them, has seen considerable progress in research and practical applications across various metal ion batteries<sup>[138]</sup>. The traditional microwave solvothermal method utilizes the penetrative nature of microwave radiation and non-contact heating to uniformly heat the solvent and reaction system in a short time. Islam *et al.* developed polypyrrole (PPy)-coated  $\text{Na}_{1.1}\text{V}_3\text{O}_{7.9}$  (P-NVO) nanorods using a microwave-assisted solvothermal approach with a reaction time of 3 h and a microwave temperature of  $180^\circ\text{C}$ , as illustrated in Figure 8A<sup>[139]</sup>. The process benefitted from the uniform heat distribution in microwave-assisted heating, leading to the even and smooth deposition of PPy on the NVO surface. The resulting smooth surface of the PPy coating is presumed to improve electron transport within the microstructure, primarily due to a significant reduction in surface roughness, which may enhance the electrochemical reaction kinetics at the interface between the electrode and the electrolyte. Compared to the uncoated NVO, the P-NVO exhibited remarkable cyclic stability and high-load endurance, maintaining its capacity without degradation after 1,100 charging and discharging cycles at a high current density of  $6,000 \text{ mA g}^{-1}$ . Figure 8B illustrates defect-rich soft carbon porous nanosheets (SC-NS) prepared by microwave-assisted liquid-phase exfoliation, employing a microwave treatment of 5 min at a power of  $300 \text{ W}$ <sup>[84]</sup>. The microwave treatment notably increased the surface area of SC-NS from  $19.1$  to  $471.2 \text{ m}^2 \text{ g}^{-1}$ .



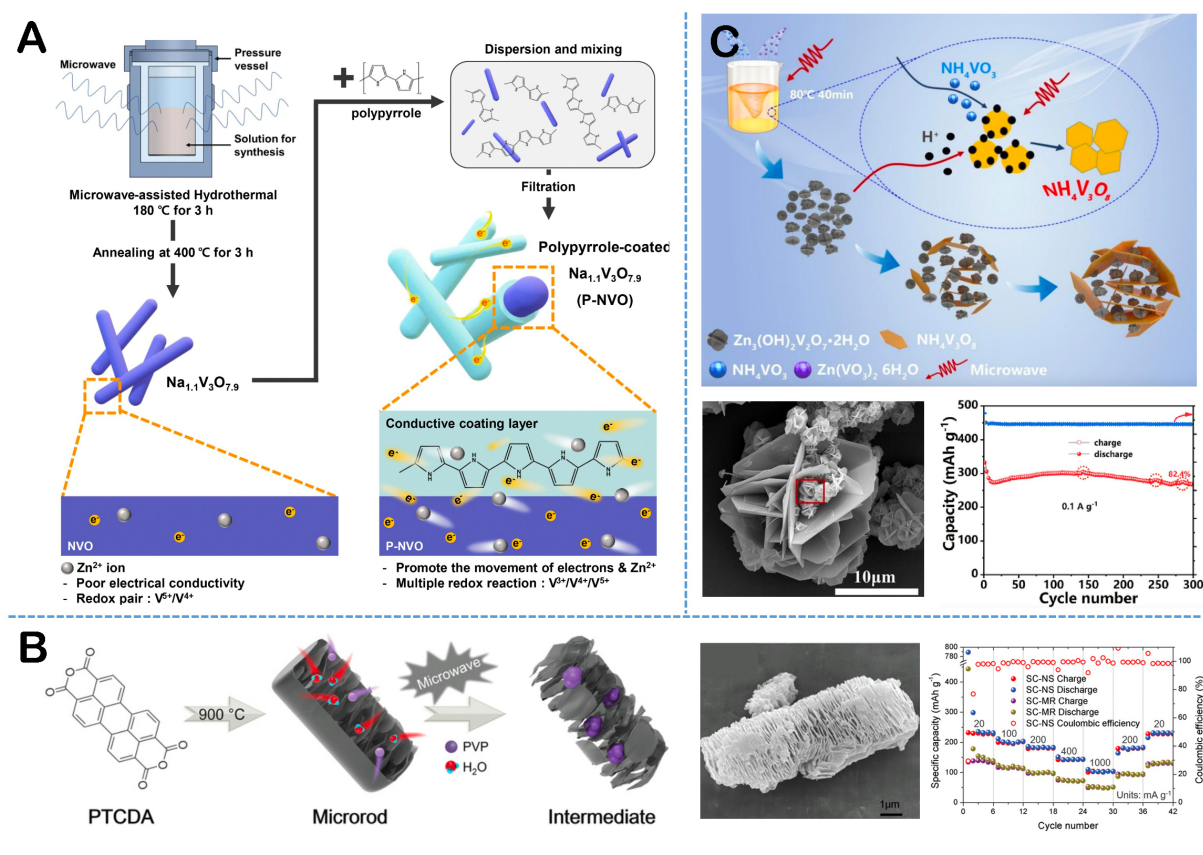


**Figure 8.** (A) PPy-coated  $\text{Na}_{1.1}\text{V}_3\text{O}_{7.9}$  nanorods prepared using the liquid-phase microwave method. This figure is quoted with permission<sup>[139]</sup>; (B) Defect-rich soft carbon porous nanosheets fabricated via the liquid-phase microwave method, emphasizing their specific capacity in sodium-ion battery applications. This figure is quoted with permission<sup>[84]</sup>; (C) 3D  $\text{NH}_4\text{V}_3\text{O}_8/\text{Zn}_3(\text{OH})_2\text{V}_2\text{O}_7 \cdot 2\text{H}_2\text{O}$  composite materials prepared using the liquid-phase microwave method, showcasing their specific capacity in zinc-ion battery applications. This figure is quoted with permission<sup>[140]</sup>.

and amplified the pore capacity more than 100 fold, while also introducing beneficial defects at the edges of the graphene layers. This expansion of the electrochemical reaction interface and additional ion storage sites result in a high specific capacity of 232 mAh g<sup>-1</sup> and excellent rate performance in sodium-ion batteries, and a reversible capacity of 291 mAh g<sup>-1</sup> in potassium-ion batteries, with outstanding rate performance of 117 mAh g<sup>-1</sup> at a current density of 2,400 mA g<sup>-1</sup>. As shown in Figure 8C, Liu *et al.* synthesized 3D  $\text{NH}_4\text{V}_3\text{O}_8/\text{Zn}_3(\text{OH})_2\text{V}_2\text{O}_7 \cdot 2\text{H}_2\text{O}$  composite material as the cathode for zinc-ion batteries using a microwave radiation-assisted chemical precipitation method<sup>[140]</sup>. This method achieves rapid and uniform heating, reduces reaction time to 40 min, lowers synthesis temperature to 80 °C, and promotes the orderly formation of  $\text{NH}_4\text{V}_3\text{O}_8$  nanosheets with  $\text{Zn}_3(\text{OH})_2\text{V}_2\text{O}_7 \cdot 2\text{H}_2\text{O}$  nanoflowers. The unique structural design of this composite enables it to exhibit a high specific capacity of 332 mAh g<sup>-1</sup> at 0.1 A g<sup>-1</sup> and a capacity retention rate of 92% after 1,000 cycles at 10 A g<sup>-1</sup>, showcasing its potential in zinc-ion battery applications. Moreover, Hou *et al.* demonstrate the successful preparation of a  $\text{Na}_3\text{V}_2(\text{PO}_4)_2\text{O}_2\text{F}/\text{C}$  composite, featuring a stratified mulberry self-assembly structure, achieved through a rapid microwave-assisted low-temperature reflux technique<sup>[86]</sup>. The process of microwave-assisted synthesis plays a pivotal role in fostering the generation of nanocomposites with a high degree of structural order. This structural order is essential for enhancing charge mobility, a key factor in improving the properties of electrode materials. When applied as a cathode



material in sodium-ion batteries, this  $\text{Na}_3\text{V}_2(\text{PO}_4)_2\text{O}_2\text{F@C}$  composite exhibited a noteworthy initial specific capacity of  $127.9 \text{ mA h g}^{-1}$  at a  $0.1 \text{ C}$  discharge rate. Therefore, microwave technology effectively promotes oriented growth in the synthesis of 1D and 2D nanomaterials, thereby enhancing ion adsorption and electron transport properties.

### Supercapacitors

Supercapacitors, with their prolonged lifespan, substantial power density, and broad operating temperature range, occupy a crucial niche in the energy storage sector<sup>[141-143]</sup>. However, they face significant challenges such as low energy density and the high cost of electrode materials, which curtail their development<sup>[144]</sup>. Addressing these challenges, particularly in enhancing the energy storage electrode materials for supercapacitors, is a formidable task. In recent years, microwave-assisted synthesis technology has garnered considerable attention in synthesizing and modifying materials for supercapacitors. This technology is adept at precisely controlling the nanoscale microstructure of electrode materials, which is key to optimizing their electrochemical properties. These improved microstructures not only have the potential to increase the energy density of capacitors but also offer prospects for reducing material costs. Consequently, the advancement of microwave-assisted synthesis is poised to significantly propel the development of supercapacitor technology, potentially overcoming current limitations and expanding their applicability in various energy storage applications.

The 0D nanostructure is pivotal in enhancing supercapacitor performance due to its high specific surface area and shortened ion transport path, which collectively boost charge storage and power density. Recent research indicates that 0D nanostructures, synthesized through microwave-assisted methods, show significant potential for supercapacitor electrode applications. As shown in Figure 9A, the work of Zhang *et al.* demonstrates the synthesis of functionalized multi-component mesoporous  $\text{Ni}_x\text{Co}_{3-x}(\text{PO}_4)_2$  hollow shell materials with diverse morphologies, including mesoporous hollow shells, pompon-shaped hierarchical shells and nanosheets<sup>[32]</sup>. This was achieved through a microwave-assisted technique, with a reaction time of 20 min at a microwave temperature of  $200^\circ\text{C}$  and power of 700 W, integrated with an oil-water microemulsion template in a hydrothermal setting, where the molar ratio of nickel to cobalt in the reaction system was meticulously regulated. The quick reaction nature of microwave synthesis not only promoted the formation of hollow shells with extensive pore structures and increased specific surface areas but also significantly improved the electrochemical performance of materials. Notably, the  $\text{NiCo}_2(\text{PO}_4)_2$  hollow shell, as an electrode material in supercapacitors, exhibited a maximum specific capacitance of  $940 \text{ F g}^{-1}$ . Relative to the conventional liquid-phase microwave synthesis, the advanced gas-phase microwave technique enables a swifter synthesis of materials. Figure 9B illustrates the successful preparation of a bismuth oxide electrode based on CNT support through microwave-assisted nanowelding technology<sup>[145]</sup>. In this process, a reaction time of 6 h, a microwave temperature of  $160^\circ\text{C}$ , and a microwave power of 800 W were employed. This approach uses microwave radiation to trigger the thermal absorption of graphene, catalyzing the conversion of glucose (as a carbon source) to form carbon dots. This mechanism effectively promotes the tight integration of graphene with  $\text{Bi}_2\text{O}_3$ , while maximally preserving the nanostructure's integrity. The graphene/carbon dot composite packaging ensures optimized electron transport away from the CNT core axis on the wrinkled graphene layer of the  $\text{CNT@Bi}_2\text{O}_3$  nanobeam surface. As a negative electrode of a supercapacitor,  $\text{CNT@Bi}_2\text{O}_3\text{-G}$  provides a high energy density of  $589.3 \text{ }\mu\text{Wh cm}^{-2}$  at a power density of  $0.8 \text{ mW cm}^{-2}$  and maintains an 80.1% capacity retention rate after 8,000 charge and discharge cycles. Figure 9C showcases the successful synthesis of a nitrogen-doped porous graphene framework (NPGF) containing 0D particles by Wang *et al.*, using *in situ* microwave-assisted rapid chain reduction technology<sup>[146]</sup>. These nanoparticles, less than 10 nm in diameter, are evenly distributed throughout the framework. Microwave treatment not only accelerated NPGF formation in just 3 to 5 s but also induced significant volume expansion of the material, from an initial thickness of 8.4 to  $904 \text{ }\mu\text{m}$ , approximately

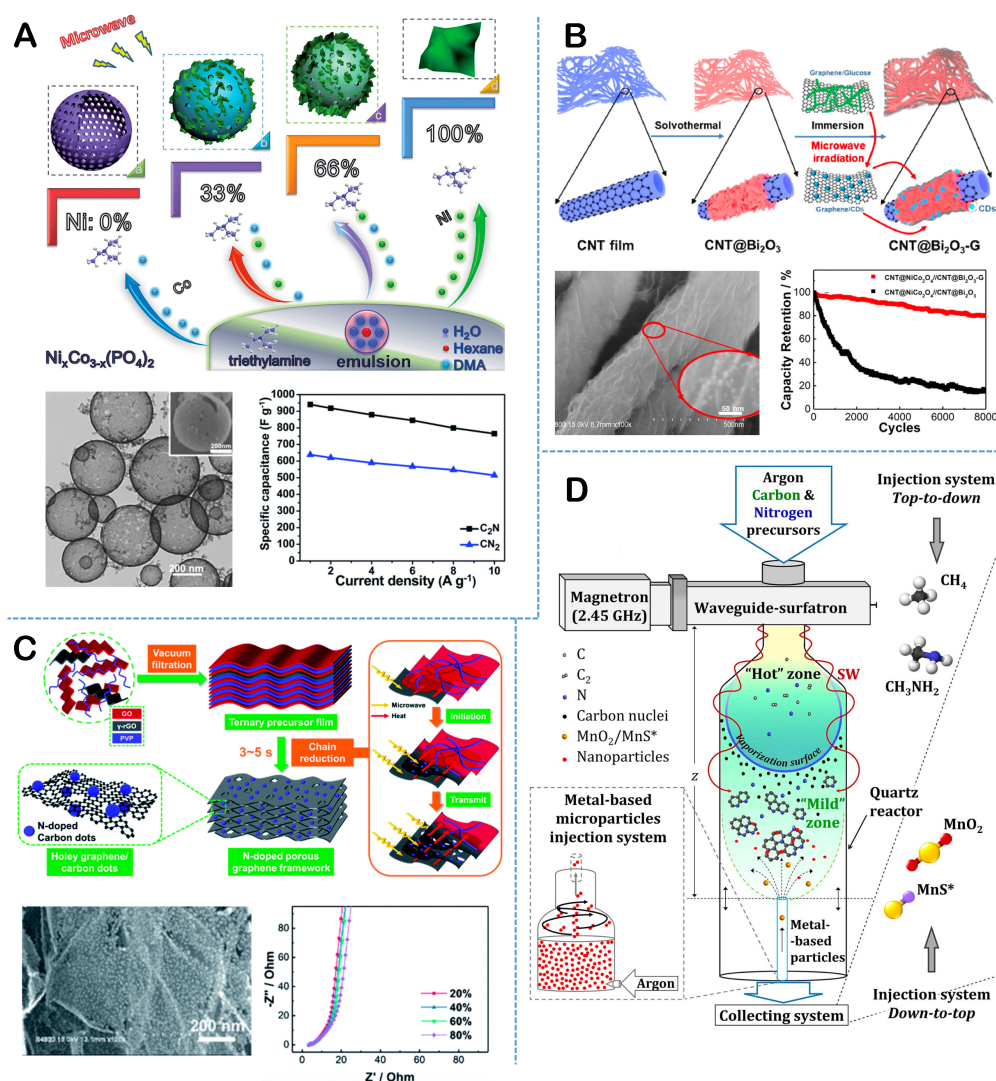


**Figure 9.** (A) Functionalized multi-component mesoporous  $\text{Ni}_x\text{Co}_{3-x}(\text{PO}_4)_2$  hollow shell materials with diverse morphologies prepared via the liquid-phase microwave method, focusing on their specific capacitance characteristics in supercapacitor applications. This figure is quoted with permission<sup>[32]</sup>; (B)  $\text{Bi}_2\text{O}_3$  prepared on CNTs using the gas-phase microwave method, emphasizing their cycle stability in supercapacitor applications. This figure is quoted with permission<sup>[145]</sup>; (C) OD nitrogen-doped porous graphene frameworks with nanoscale particles, fabricated using the gas-phase microwave method, showcasing their high energy density characteristics in supercapacitor applications. This figure is quoted with permission<sup>[146]</sup>; (D) Metal oxides and metal sulfide nanoparticles prepared on nitrogen-doped graphene via the gas-phase microwave method. This figure is quoted with permission<sup>[36]</sup>.

100 times the thickness of the original precursor film. In supercapacitor applications, NPGF achieves a high volume energy density of  $12.3 \text{ mWh cm}^{-3}$  at a power density of  $0.42 \text{ W cm}^{-3}$  and maintains 90.2% capacity after 20,000 charge and discharge cycles, demonstrating its potential in high-performance supercapacitor technologies. In Figure 9D, the work of Dias *et al.* is showcased, where they have adeptly synthesized N-graphene-metal-oxide (sulfide) hybrid nanostructures, using a single-step microwave plasma-assisted process<sup>[36]</sup>. This process utilized a substantial microwave power of 2 kW at a frequency of 2.45 GHz. During this synthesis phase, the microwave plasma, within its high-energy density zones, emitted energy and atomic and molecular particles (such as C,  $\text{C}_2$ , N, CN). This emission drove these particles towards the lower energy density afterglow region of the plasma, which, in turn, promoted the assembly and growth of the nitrogen-doped graphene sheets. Moreover, the process involved the reverse injection of micron-sized

metal particles, leading to their size reduction and subsequent anchoring on the growing nitrogen-doped graphene sheets. In the context of supercapacitor applications, these N-graphene-metal-oxide hybrid nanostructures demonstrated remarkable electrochemical stability, retaining 88% of their original specific capacitance even after 4,000 charging and discharging cycles. Therefore, nanoparticles synthesized through microwave methods typically have a higher specific surface area, which helps to provide more sites for charge storage.

In the realm of supercapacitor electrode material design, 1D nanowires and 2D nanosheets are particularly valuable due to their excellent specific surface area. This characteristic substantially increases the density of effective active sites, greatly enhancing the adsorption of electrolyte ions on the electrode surface, which is crucial for improving the capacitive performance of capacitors. Microwave-assisted synthesis processes offer a simple, efficient, and controlled means of synthesizing 1D and 2D nanomaterials, thereby ensuring their exceptional performance in supercapacitors. For instance, Sun *et al.* employed a microwave-assisted solvothermal method to fabricate 1D porous CoO nanowire arrays for binder-free supercapacitor electrodes<sup>[147]</sup>. The microwave-assisted process notably enhanced the purity of the synthetic precursor and induced a change in the crystal structure. Compared to conventional synthesis methods, these microwave-assisted porous CoO nanowires exhibited a significantly improved specific capacitance. Particularly notable was the specific capacitance at a current density of 1 A g<sup>-1</sup>, which reached 728.8 F g<sup>-1</sup>, marking a substantial improvement over the reference value of 503.7 F g<sup>-1</sup>. In contrast to the microwave solvothermal approach, the solid-phase microwave technique allows for direct treatment of solids without solvents, which minimizes the likelihood of by-products in the reaction process. Figure 10A displays the carbon-bridged Nb<sub>2</sub>O<sub>5</sub> mesocrystals created using the solid-phase microwave-assisted synthesis method, intended for use in sodium-ion capacitors<sup>[148]</sup>. In the synthesis process, which involves a reaction time of 4 min at a microwave power of 800 W, the “hotspots” created by microwave energy accelerate the decomposition of Nb-oxalate and the reorganization of Nb(V) cations, forming 1D carbon-bridged single-crystal nanorods. This distinctive structural configuration imparts the material with a notably high specific capacity, reaching up to 133.4 mA h g<sup>-1</sup>. Within the realm of supercapacitors, 1D materials are significantly influential in terms of their key performance attributes, whereas 2D materials equally assume an essential role. Figure 10B illustrates the synthesis of ultra-large and thin NiAl layered bimetallic hydroxide nanosheets, uniformly grown on graphene surfaces, achieved through a microwave-assisted solvothermal method<sup>[149]</sup>. These nanosheets, as electrode materials for supercapacitors, enhance the specific surface area of the electrodes, which is instrumental in improving their capacitance characteristics. When tested at a current density of 1 A g<sup>-1</sup>, the composite demonstrates a remarkable specific capacitance of 1,055 F g<sup>-1</sup>. Figure 10C illustrates the work of Rafai *et al.*, who adeptly prepared non-layered ultrathin CoNi<sub>2</sub>S<sub>4</sub> nanosheets at room temperature using microwave-assisted liquid-phase growth technology<sup>[60]</sup>. When these nanosheets were applied as cathode materials in hybrid supercapacitors, they achieved a high energy density of 67.7 Wh kg<sup>-1</sup> at a power density of 0.8 kW kg<sup>-1</sup>. Furthermore, they maintained an energy density of 50.6 Wh kg<sup>-1</sup> at higher power densities. This performance demonstrates the potential of microwave-assisted synthesis in creating advanced materials for high-energy-density supercapacitors. Compared to traditional liquid-phase microwave synthesis, advanced solid-phase microwave technology offers more pronounced advantages in synthesizing complex micro-nanostructures. For instance, as shown in Figure 10D, Lin *et al.* utilized microwave-assisted solid-phase synthesis technology, with a reaction time of 6 min at a microwave power of 200 W and a temperature of 65 °C, to prepare a novel core-shell heterostructure, with multi-walled CNT as the core and graphene oxide nanoribbons as the shell (MWCNT@GONR)<sup>[150]</sup>. The microwave energy-assisted MWCNT open-chain technology not only opens up the MWCNTs but also facilitates the growth of graphene oxide nanoribbons on their surface to form a unique core-shell structure. This structure combines the tubular properties of MWCNTs with the layered structure of graphene oxide. When utilized as electrode materials for supercapacitors, MWCNT@GONR significantly enhances specific capacitance, reaching



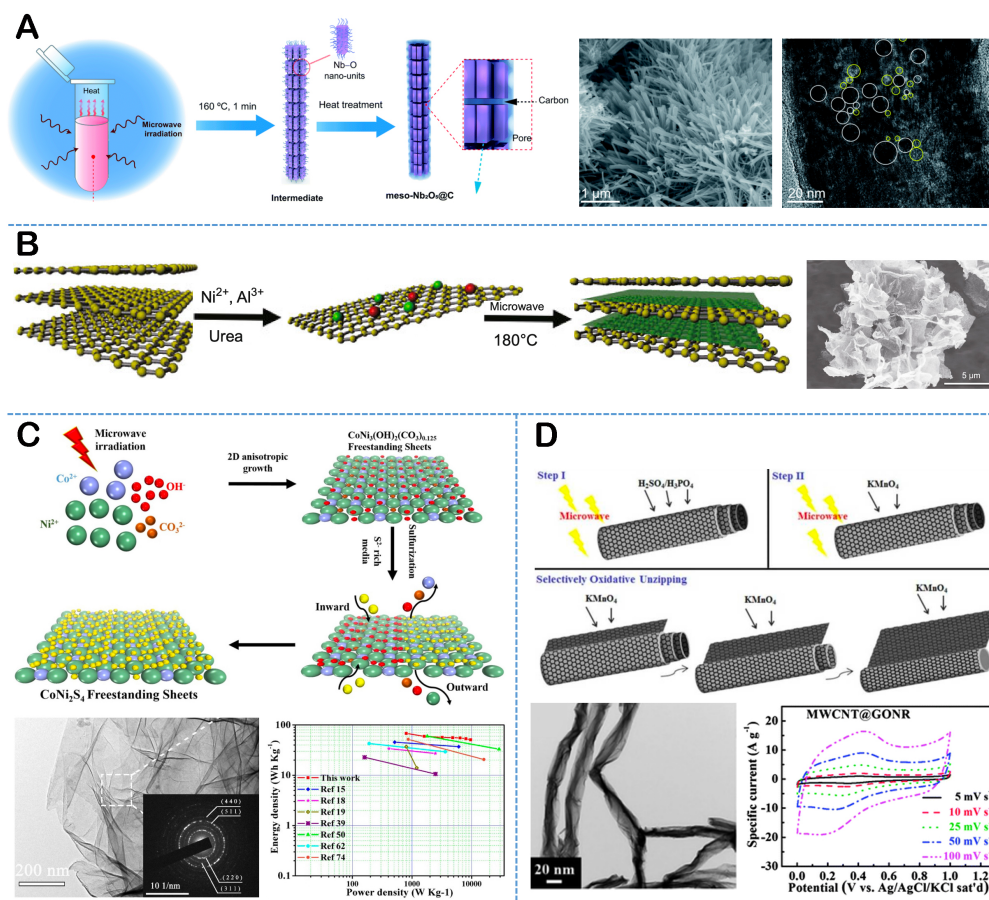


**Figure 10.** (A) 1D carbon-bridged Nb<sub>2</sub>O<sub>5</sub> single-crystal nanorods prepared using the solid-phase microwave method. This figure is quoted with permission<sup>[148]</sup>; (B) Ultra-large and thin NiAl layered bimetallic hydroxide nanosheets fabricated via the liquid-phase microwave method. This figure is quoted with permission<sup>[149]</sup>; (C) Non-layered ultrathin CoNi<sub>2</sub>S<sub>4</sub> nanosheets prepared using the liquid-phase microwave method, emphasizing their high energy density characteristics in supercapacitor applications. This figure is quoted with permission<sup>[60]</sup>; (D) Nanocomposite materials MWCNT@GONR prepared through the solid-phase microwave method, focusing on their specific capacitance characteristics in supercapacitor applications. This figure is quoted with permission<sup>[150]</sup>.

252.4 F g<sup>-1</sup>. In microwave-assisted synthesis, 1D nanomaterials exhibit enhanced mechanical stability, crucial for the long-term performance of supercapacitors. Moreover, this method also expands the interlayer spacing of 2D materials, accelerating ion exchange and optimizing electrochemical performance.

Microwave-assisted material modification technology plays a crucial role in enhancing the performance of supercapacitor electrode materials by optimizing nanostructure characteristics, such as controlling doping levels and defect formation. Using a rapid microwave-assisted solvothermal technique, Gupta *et al.* successfully synthesized titanium phosphate-free phosphorus-doped Ti<sub>3</sub>C<sub>2</sub> MXene, effectively preventing the unintended formation of titanium phosphate phases common in traditional heating doping processes. The process involved optimizing microwave irradiation at power settings from 500 to 1,000 W and durations from 30 s to 5 min under a controlled temperature of 60 °C, as shown in Figure 11A<sup>[151]</sup>. The doping with phosphorus increases interlayer distance in the material, an essential structural modification for promoting small H<sup>+</sup> ion intercalation activities in electrochemical energy storage, consequently augmenting the energy storage capabilities of the material. The fabricated phosphorus-doped Ti<sub>3</sub>C<sub>2</sub>, free from titanium phosphate, exhibited an impressive specific capacitance reaching 1,702 F cm<sup>-3</sup> g<sup>-1</sup>. Figure 11B

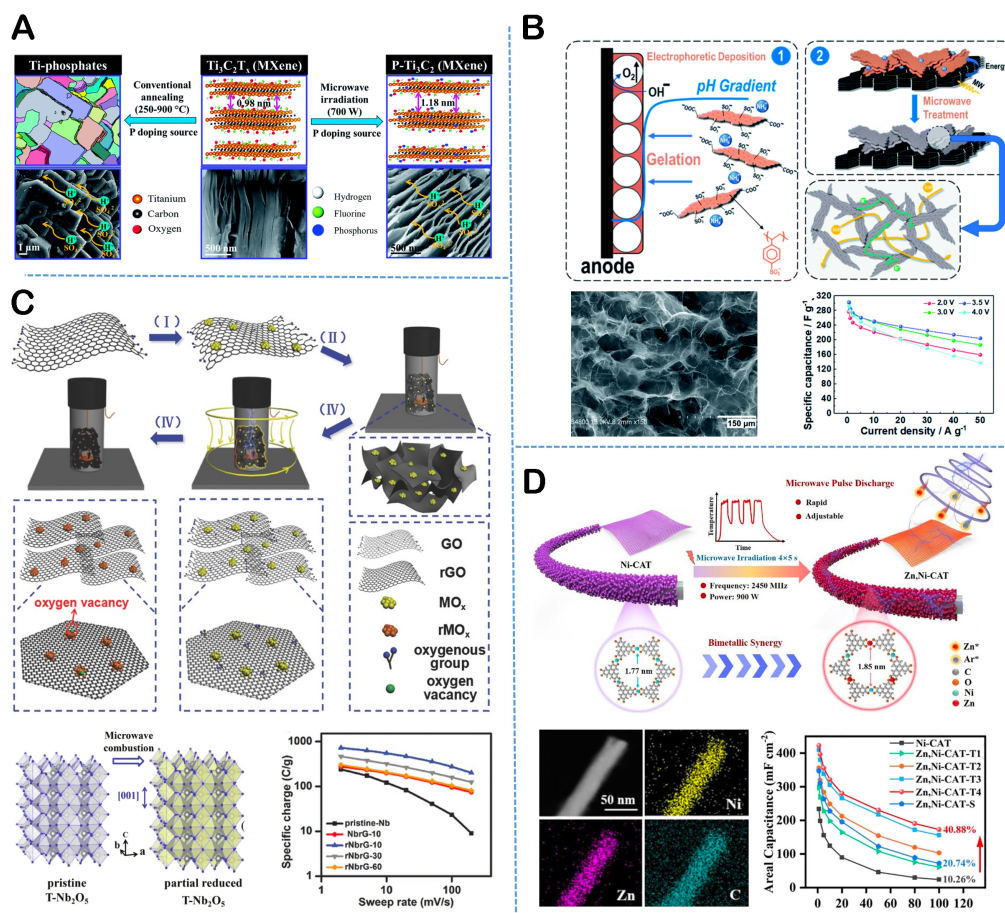


**Figure 11.** (A) Titanium phosphate-free phosphorus-doped  $\text{Ti}_3\text{C}_2$  MXene prepared using the liquid-phase microwave method. This figure is quoted with permission<sup>[151]</sup>; (B) Sulfurs, nitrogen-doped graphene foam fabricated via the liquid-phase microwave method, focusing on their specific capacitance characteristics in supercapacitor applications. This figure is quoted with permission<sup>[152]</sup>; (C) Introduction of oxygen vacancies in transition metal oxides using the microwave combustion method and their reversible specific capacity characteristics in supercapacitor applications. This figure is quoted with permission<sup>[34]</sup>; (D) Rapid introduction of bimetallic zinc and nickel-catecholate complexes in MOFs using a vapor-phase microwave pulse discharge strategy, highlighting their specific capacitance characteristics in supercapacitor applications. This figure is quoted with permission<sup>[95]</sup>.

illustrates the preparation of sulfur, nitrogen-doped graphene foam (dGF) on ultrathin graphite paper using electrophoretic deposition and microwave reduction for a brief duration of 5 s<sup>[152]</sup>. The dGF, characterized by a high specific surface area (1,806 m<sup>2</sup> g<sup>-1</sup>) and dual doping with sulfur and nitrogen, exhibits high specific capacitance (354 F g<sup>-1</sup>) and excellent rate performance. Using graphite paper as the deposition substrate and microwave as the reducing agent simplifies the preparation of the digital interelectrode. The resulting flexible supercapacitor maintains 99.5% of its specific capacitance after 10,000 charge and discharge cycles at a power density of 0.65 kW kg<sup>-1</sup>, and an energy density of 71.5 Wh kg<sup>-1</sup>. Compared to traditional liquid-phase microwave techniques, advanced solid-phase and gas-phase microwave synthesis methods demonstrate significant superiority in reducing synthesis cycles, minimizing risks of acid and base corrosion, and enhancing the universality and controllability of material synthesis. Figure 11C features the work of Wan *et al.*, who employed microwave combustion to introduce oxygen vacancies into transition metal oxides such as  $\text{V}_2\text{O}_5$ ,  $\text{WO}_3$ ,  $\text{TiO}_2$ , and  $\text{Nb}_2\text{O}_5$ , aiming to enhance their electrochemical performance<sup>[34]</sup>. The reduced  $\text{Nb}_2\text{O}_5$  ( $\text{rNb}_2\text{O}_5$ ) material synthesized in this process exhibited an increased interlayer distance, facilitating accelerated ion diffusion rates. Notably, the composite combining  $\text{rNb}_2\text{O}_5$  and rGO



demonstrated exceptional electrochemical properties in an organic electrolyte. It achieved a reversible specific capacity of  $726.2 \text{ C g}^{-1}$  at a scan rate of  $2 \text{ mV s}^{-1}$  and maintained 87% capacity even after 3,000 charge and discharge cycles, indicating outstanding cyclic stability. Figure 11D demonstrates our team's development of a vapor-phase microwave pulse discharge strategy, enabling the rapid and controlled synthesis of high-performance, stable bimetallic Zn,Ni-catecholate (Zn,Ni-CAT) by sputtering high-energy zinc particles onto conductive Ni-CAT<sup>[95]</sup>. This method drastically reduces the synthesis time to a mere 20 s, surpassing many constraints of the traditional solvothermal technique. When used as a supercapacitor electrode material, it exhibits a superior specific capacitance of  $422.54 \text{ mF cm}^{-2}$  and maintains 91.53% of its cycle stability even after 30,000 charging and discharging cycles. Therefore, microwave technology demonstrates significant potential in the functionalization of material surfaces, especially in introducing specific functional groups or active sites, which is crucial for modulating the hydrophilicity or electrophilicity of electrode materials.

## CONCLUSIONS AND OUTLOOK

In the field of energy storage material science, the precise design and synthesis of materials with specific structures and morphologies are crucial for enhancing the performance of energy storage devices. This article reviews the significant advancements in preparing energy storage materials with specific microstructures and morphologies using advanced microwave-assisted synthesis techniques. We found that microwave-assisted synthesis is particularly effective in optimizing the microstructures of energy storage electrode materials. Specifically, this method has unique advantages in controlling material dimensions, precisely controlling grain sizes, designing specific crystal configurations, and implementing defect engineering. These optimizations have improved the electrochemical performance of the materials, including increased specific capacitance, improved electrical conductivity, and enhanced cycle stability. Particularly in fields such as lithium-ion batteries and supercapacitors, microwave technology has greatly enriched the performance and application range of electrode materials.

Advanced microwave-assisted synthesis techniques show significant advantages in preparing energy storage electrode materials. A key feature of this technique is the rapid heating of precursors to high temperatures ( $600\text{--}1,000 \text{ }^{\circ}\text{C}$ ) in a high-energy microwave environment. This rapid heating and cooling characteristic perfectly avoids the formation of by-products or phase changes due to temperature gradients during heating and cooling. Moreover, the rapid heating process helps to prevent crystal overgrowth or structural damage that might occur during long-term high-temperature treatment, thereby facilitating the synthesis of purer materials with specific microstructures. Another significant feature of this technology is the substantial reduction in reaction time; for example, the materials synthesis can be completed within a few seconds to minutes, greatly improving experimental efficiency and reducing energy consumption compared to traditional thermal treatment methods. Additionally, it is important to address the safety aspects related to EMR in microwave-assisted synthesis. Modern microwave systems are designed with effective shielding, ensuring that they operate within safe EMR levels according to international standards and thereby mitigating significant health risks or environmental impacts. The non-ionizing nature of microwave radiation also contributes to the environmental friendliness of this method. Lastly, the environmental friendliness and energy efficiency of advanced microwave-assisted synthesis technology are also noteworthy. As this method does not require solvents, it is not only more environmentally friendly but also reduces the use of harmful solvents, aligning with the principles of green chemistry. Developing this synthesis technology provides an efficient, sustainable new pathway for synthesizing energy storage electrode materials, having significant research implications in materials science.

Despite the significant advantages of microwave-assisted synthesis in the synthesis of energy storage materials, there remain challenges in its application.

(1) Due to the lack of precise temperature measurement, the widespread industrial application of microwave-assisted synthesis remains unattained. The development of affordable and accurate temperature measurement systems could facilitate the transition of this technology from laboratory to industrial applications, significantly enhancing the feasibility and popularity of microwave synthesis techniques.

(2) Current microwave synthesis technology faces production scale limitations, particularly in milligram-level single batch processes. To achieve a substantial increase in daily production capacity, it is crucial to optimize synthesis pathways and enhance separation and purification efficiency. Furthermore, newly developed microwave reactors, such as intensified multiphase reactors, may offer an effective means to improve product selectivity and productivity. These advanced devices can more effectively control reaction conditions, thereby increasing yield and product quality.

(3) Establishing a precise mechanism of microwave heating is key to enhancing the efficiency of microwave synthesis. Future efforts should involve more detailed theoretical analysis and modeling simulations to gain a deeper understanding of microwave heating characteristics. Additionally, intelligent control of chemical reactions during microwave heating can improve product yield and quality.

(4) Microwave technology has proven advantageous in fabricating porous electrodes and batteries. However, issues such as forming solid electrolyte interphases in lithium-ion batteries need to be rapidly addressed. Also, increasing the energy density of supercapacitors remains a focus for future research.

## **DECLARATIONS**

### **Authors' contributions**

Conceptualization: Wan J, You Y, Fang G

Formal analysis and software: You Y, Guo J, Li Q

Data curation and writing-original draft: You Y, Fang G, Fan M

Funding acquisition, supervision, validation and writing-review & editing: Wan J

### **Availability of data and materials**

Not applicable.

### **Financial support and sponsorship**

This work is supported by the National Natural Science Foundation of China (52203070) and the Open Fund of Hubei Key Laboratory of Biomass Fiber and Ecological Dyeing and Finishing (STRZ202203). Wan J expresses gratitude for the financial support provided by the China Scholarship Council (CSC) Visiting Scholar Program.

### **Conflicts of interest**

All authors declared that there are no conflicts of interest.

### **Ethical approval and consent to participate**

Not applicable.

## Consent for publication

Not applicable.

## Copyright

© The Author(s) 2024.

## REFERENCES

1. Zhao Y, Jin B, Zheng Y, Jin H, Jiao Y, Qiao S. Charge state manipulation of cobalt selenide catalyst for overall seawater electrolysis. *Adv Energy Mater* 2018;8:1801926. [DOI](#)
2. Li L, Tang C, Jin H, Davey K, Qiao S. Main-group elements boost electrochemical nitrogen fixation. *Chem* 2021;7:3232-55. [DOI](#)
3. Jacobson MZ, von Krauland A, Coughlin SJ, et al. Low-cost solutions to global warming, air pollution, and energy insecurity for 145 countries. *Energy Environ Sci* 2022;15:3343-59. [DOI](#)
4. Ding Y, Mu C, Wu T, et al. Increasing cryospheric hazards in a warming climate. *Earth Sci Rev* 2021;213:103500. [DOI](#)
5. Yao D, Tang C, Wang P, et al. Electrocatalytic green ammonia production beyond ambient aqueous nitrogen reduction. *Chem Eng Sci* 2022;257:117735. [DOI](#)
6. Yu H, Wan J, Goodsite M, Jin H. Advancing direct seawater electrocatalysis for green and affordable hydrogen. *One Earth* 2023;6:267-77. [DOI](#)
7. Chen P, Hou J, Wang L. Metal-organic framework-tailored perovskite solar cells. *Microstructures* 2022;2:2022014. [DOI](#)
8. Ragauskas AJ, Williams CK, Davison BH, et al. The path forward for biofuels and biomaterials. *Science* 2006;311:484-9. [DOI](#)
9. Armand M, Tarascon JM. Building better batteries. *Nature* 2008;451:652-7. [DOI](#) [PubMed](#)
10. Dunn B, Kamath H, Tarascon JM. Electrical energy storage for the grid: a battery of choices. *Science* 2011;334:928-35. [DOI](#) [PubMed](#)
11. Sun H, Mei L, Liang J, et al. Three-dimensional holey-graphene/niobia composite architectures for ultrahigh-rate energy storage. *Science* 2017;356:599-604. [DOI](#)
12. Chen K, Xue D. Materials chemistry toward electrochemical energy storage. *J Mater Chem A* 2016;4:7522-37. [DOI](#)
13. Ji X, Lee KT, Nazar LF. A highly ordered nanostructured carbon-sulphur cathode for lithium-sulphur batteries. *Nat Mater* 2009;8:500-6. [DOI](#) [PubMed](#)
14. Sumboja A, Liu J, Zheng WG, Zong Y, Zhang H, Liu Z. Electrochemical energy storage devices for wearable technology: a rationale for materials selection and cell design. *Chem Soc Rev* 2018;47:5919-45. [DOI](#) [PubMed](#)
15. Zhang L, Zhou K, Wei Q, et al. Thermal conductivity enhancement of phase change materials with 3D porous diamond foam for thermal energy storage. *Appl Energy* 2019;233-4:208-19. [DOI](#)
16. Raj CJ, Manikandan R, Thondaiman P, et al. Sonochemical exfoliation of graphene in various electrolytic environments and their structural and electrochemical properties. *Carbon* 2021;184:266-76. [DOI](#)
17. Lee SJ, Kim HJ, Hwang TH, et al. Delicate structural control of Si-SiO<sub>x</sub>-C composite via high-speed spray pyrolysis for Li-ion battery anodes. *Nano Lett* 2017;17:1870-6. [DOI](#)
18. Zhang X, Zhang W, Zhang L, et al. Single-pot solvothermal strategy toward support-free nanostructured LiBH<sub>4</sub> featuring 12 wt% reversible hydrogen storage at 400 °C. *Chem Eng J* 2022;428:132566. [DOI](#)
19. Li Y, Liu H, Xu J, et al. Hierarchical nanostructure-tuned super-high electrochemical stability of nickel cobalt sulfide. *J Mater Chem A* 2018;6:19788-97. [DOI](#)
20. Carriazo D, Rossell MD, Zeng G, Bilecka I, Erni R, Niederberger M. Formation mechanism of LiFePO<sub>4</sub> sticks grown by a microwave-assisted liquid-phase process. *Small* 2012;8:2231-8. [DOI](#) [PubMed](#)
21. Wan J, Zhang G, Jin H, et al. Microwave-assisted synthesis of well-defined nitrogen doping configuration with high centrality in carbon to identify the active sites for electrochemical hydrogen peroxide production. *Carbon* 2022;191:340-9. [DOI](#)
22. Fang G, Liu K, Fan M, et al. Unveiling the electron configuration-dependent oxygen evolution activity of 2D porous Sr-substituted LaFeO<sub>3</sub> perovskite through microwave shock. *Carbon Neutral* 2023;2:709-20. [DOI](#)
23. Strauss V, Marsh K, Kowal MD, El-Kady M, Kaner RB. A simple route to porous graphene from carbon nanodots for supercapacitor applications. *Adv Mater* 2018;30:1704449. [DOI](#) [PubMed](#)
24. Jiang H, Li J, Xiao Z, et al. The rapid production of multiple transition metal carbides via microwave combustion under ambient conditions. *Nanoscale* 2020;12:16245-52. [DOI](#)
25. Hu R, Wei L, Xian J, et al. Microwave shock process for rapid synthesis of 2D porous La<sub>0.2</sub>Sr<sub>0.8</sub>CoO<sub>3</sub> perovskite as an efficient oxygen evolution reaction catalyst. *Acta Physico Chim Sinica* 2023;0:2212025. [DOI](#)
26. Wan J, Huang L, Wu J, et al. Rapid synthesis of size-tunable transition metal carbide nanodots under ambient conditions. *J Mater Chem A* 2019;7:14489-95. [DOI](#)
27. Xian J, Jiang H, Wu Z, et al. Microwave shock motivating the Sr substitution of 2D porous GdFeO<sub>3</sub> perovskite for highly active oxygen evolution. *J Energy Chem* 2024;88:232-41. [DOI](#)
28. Hu R, Jiang H, Xian J, et al. Microwave-pulse sugar-blowing assisted synthesis of 2D transition metal carbides for sustainable hydrogen evolution. *Appl Catal B Environ* 2022;317:121728. [DOI](#)

29. Wang C, Xu J, Yuen M, et al. Hierarchical composite electrodes of nickel oxide nanoflake 3D graphene for high-performance pseudocapacitors. *Adv Funct Mater* 2014;24:6372-80. DOI
30. Zhang Y, Yang S, Wang S, Liu X, Li L. Microwave/freeze casting assisted fabrication of carbon frameworks derived from embedded upholder in tremella for superior performance supercapacitors. *Energy Stor Mater* 2019;18:447-55. DOI
31. Kheradmandfard M, Minouei H, Tsvetkov N, et al. Ultrafast green microwave-assisted synthesis of high-entropy oxide nanoparticles for Li-ion battery applications. *Mater Chem Phys* 2021;262:124265. DOI
32. Zhang J, Yang Y, Zhang Z, Xu X, Wang X. Rapid synthesis of mesoporous  $\text{Ni}_x\text{Co}_{3-x}(\text{PO}_4)_2$  hollow shells showing enhanced electrocatalytic and supercapacitor performance. *J Mater Chem A* 2014;2:20182-8. DOI
33. Zheng W, Zhang P, Chen J, Tian WB, Zhang Y, Sun ZM. *In situ* synthesis of CNTs@ $\text{Ti}_3\text{C}_2$  hybrid structures by microwave irradiation for high-performance anodes in lithium ion batteries. *J Mater Chem A* 2018;6:3543-51. DOI
34. Wan J, Yao X, Gao X, et al. Microwave combustion for modification of transition metal oxides. *Adv Funct Mater* 2016;26:7263-70. DOI
35. Wan J, Hu R, Li J, et al. A universal construction of robust interface between 2D conductive polymer and cellulose for textile supercapacitor. *Carbohydr Polym* 2022;284:119230. DOI
36. Dias A, Bundaleska N, Felizardo E, et al. N-graphene-metal-oxide(sulfide) hybrid nanostructures: single-step plasma-enabled approach for energy storage applications. *Chem Eng J* 2022;430:133153. DOI
37. Jessl S, Copic D, Engelke S, Ahmad S, De Volder M. Hydrothermal coating of patterned carbon nanotube forest for structured lithium-ion battery electrodes. *Small* 2019;15:e1901201. DOI PubMed
38. Liu Q, Tan G, Wang P, et al. Revealing mechanism responsible for structural reversibility of single-crystal  $\text{VO}_2$  nanorods upon lithiation/delithiation. *Nano Energy* 2017;36:197-205. DOI
39. Wang Z, Zhu Y, Qiao C, et al. Anionic Se-substitution toward high-performance  $\text{CuS}_{1-x}\text{Se}_x$  nanosheet cathode for rechargeable magnesium batteries. *Small* 2019;15:e1902797. DOI
40. Heuser S, Yang N, Hof F, Schulte A, Schönherr H, Jiang X. 3D 3C-SiC/graphene hybrid nanolaminate films for high-performance supercapacitors. *Small* 2018;14:e1801857. DOI PubMed
41. Li N, Song H, Cui H, Wang C. Sn@graphene grown on vertically aligned graphene for high-capacity, high-rate, and long-life lithium storage. *Nano Energy* 2014;3:102-12. DOI
42. Tsai W, Lin R, Murali S, et al. Outstanding performance of activated graphene based supercapacitors in ionic liquid electrolyte from -50 to 80 °C. *Nano Energy* 2013;2:403-11. DOI
43. Su X, Ye C, Li X, et al. Heterogeneous stacking carbon films for optimized supercapacitor performance. *Energy Stor Mater* 2022;50:365-72. DOI
44. Ji H, Liu C, Wang T, et al. Porous hybrid composites of few-layer  $\text{MoS}_2$  nanosheets embedded in a carbon matrix with an excellent supercapacitor electrode performance. *Small* 2015;11:6480-90. DOI
45. Zhang W, Zheng Z, Lin L, et al. Ultrafast synthesis of graphene-embedded cyclodextrin-metal-organic framework for supramolecular selective absorbency and supercapacitor performance. *Adv Sci* 2023;10:e2304062. DOI PubMed PMC
46. Li C, Shen M, Hu B, et al. High-energy nanostructured  $\text{Na}_3\text{V}_2(\text{PO}_4)_2\text{O}_{1.6}\text{F}_{1.4}$  cathodes for sodium-ion batteries and a new insight into their redox chemistry. *J Mater Chem A* 2018;6:8340-8. DOI
47. Li N, Song H, Cui H, Yang G, Wang C. Self-assembled growth of Sn@CNTs on vertically aligned graphene for binder-free high Li-storage and excellent stability. *J Mater Chem A* 2014;2:2526-37. DOI
48. Antitomaso P, Fraisse B, Stievano L, et al. SnSb electrodes for Li-ion batteries: the electrochemical mechanism and capacity fading origins elucidated by using operando techniques. *J Mater Chem A* 2017;5:6546-55. DOI
49. Kumar A, Kuang Y, Liang Z, Sun X. Microwave chemistry, recent advancements, and eco-friendly microwave-assisted synthesis of nanoarchitectures and their applications: a review. *Mater Today Nano* 2020;11:100076. DOI
50. Zhu YJ, Chen F. Microwave-assisted preparation of inorganic nanostructures in liquid phase. *Chem Rev* 2014;114:6462-555. DOI PubMed
51. Mishra RR, Sharma AK. Microwave-material interaction phenomena: heating mechanisms, challenges and opportunities in material processing. *Compos Part A Appl S* 2016;81:78-97. DOI
52. Zeng X, Cheng X, Yu R, Stucky GD. Electromagnetic microwave absorption theory and recent achievements in microwave absorbers. *Carbon* 2020;168:606-23. DOI
53. Schwenke AM, Hoeppner S, Schubert US. Synthesis and modification of carbon nanomaterials utilizing microwave heating. *Adv Mater* 2015;27:4113-41. DOI PubMed
54. Kappe CO. Controlled microwave heating in modern organic synthesis. *Angew Chem Int Ed* 2004;43:6250-84. DOI PubMed
55. Kitchen HJ, Vallance SR, Kennedy JL, et al. Modern microwave methods in solid-state inorganic materials chemistry: from fundamentals to manufacturing. *Chem Rev* 2014;114:1170-206. DOI
56. Gabriel C, Gabriel S, Grant EH, Halstead BSJ, Mingos DMP. Dielectric parameters relevant to microwave dielectric heating. *Chem Soc Rev* 1998;27:213-24. DOI
57. Baghbanzadeh M, Carbone L, Cozzoli PD, Kappe CO. Microwave-assisted synthesis of colloidal inorganic nanocrystals. *Angew Chem Int Ed* 2011;50:11312-59. DOI PubMed
58. Wang J, Wu W, Kondo H, Fan T, Zhou H. Recent progress in microwave-assisted preparations of 2D materials and catalysis applications. *Nanotechnology* 2022;33:342002. DOI



59. Zhu Y, Cao C, Zhang J, Xu X. Two-dimensional ultrathin  $\text{ZnCo}_2\text{O}_4$  nanosheets: general formation and lithium storage application. *J Mater Chem A* 2015;3:9556-64. DOI
60. Rafai S, Qiao C, Naveed M, et al. Microwave-anion-exchange route to ultrathin cobalt-nickel-sulfide nanosheets for hybrid supercapacitors. *Chem Eng J* 2019;362:576-87. DOI
61. Wu Y, Cao T, Wang R, Meng F, Zhang J, Cao C. A general strategy for the synthesis of two-dimensional holey nanosheets as cathodes for superior energy storage. *J Mater Chem A* 2018;6:8374-81. DOI
62. Li N, Liao S, Sun Y, Song HW, Wang CX. Uniformly dispersed self-assembled growth of  $\text{Sb}_2\text{O}_3/\text{Sb}@$ graphene nanocomposites on a 3D carbon sheet network for high Na-storage capacity and excellent stability. *J Mater Chem A* 2015;3:5820-8. DOI
63. Alshareef SF, Alhebshi NA, Almashhori K, Alshaikheid HS, Al-Hazmi F. A ten-minute synthesis of  $\alpha\text{-Ni}(\text{OH})_2$  nanoflakes assisted by microwave on flexible stainless-steel for energy storage devices. *Nanomaterials* 2022;12:1911. DOI PubMed PMC
64. Fathy M, Hassan H, Hafez H, Soliman M, Abulfotuh F, Kashyout AEHB. Simple and fast microwave-assisted synthesis methods of nanocrystalline  $\text{TiO}_2$  and rGO materials for low-cost metal-free DSSC applications. *ACS Omega* 2022;7:16757-65. DOI PubMed PMC
65. Rao RP, Ramasubramanian B, Saritha R, Ramakrishna S. Microwave assisted synthesis for  $\epsilon\text{-MnO}_2$  nanostructures on Ni foam as for rechargeable Li- $\text{O}_2$  battery applications. *Nano Express* 2023;4:045004. DOI
66. Iqbal M, Saykar NG, Mahapatra SK. Microwave-induced rapid synthesis of  $\text{MoS}_2@$ Cellulose composites as an efficient electrode material for quasi-solid-state supercapacitor application. *Adv Eng Mater* 2023;25:2201544. DOI
67. Soin N, Roy SS, Mitra SK, Thundat T, McLaughlin JA. Nanocrystalline ruthenium oxide dispersed few layered graphene (FLG) nanoflakes as supercapacitor electrodes. *J Mater Chem* 2012;22:14944-50. DOI
68. Wang W, Zhang N, Shi Z, et al. Preparation of Ni-Al layered double hydroxide hollow microspheres for supercapacitor electrode. *Chem Eng J* 2018;338:55-61. DOI
69. Zhu J, Chen M, Wei H, et al. Magnetocapacitance in magnetic microtubular carbon nanocomposites under external magnetic field. *Nano Energy* 2014;6:180-92. DOI
70. He G, Li L, Manthiram A.  $\text{VO}_2/\text{rGO}$  nanorods as a potential anode for sodium- and lithium-ion batteries. *J Mater Chem A* 2015;3:14750-8. DOI
71. Antiohos D, Romano MS, Razal JM, et al. Performance enhancement of single-walled nanotube-microwave exfoliated graphene oxide composite electrodes using a stacked electrode configuration. *J Mater Chem A* 2014;2:14835-43. DOI
72. Murali S, Quarles N, Zhang LL, et al. Volumetric capacitance of compressed activated microwave-expanded graphite oxide (a-MEGO) electrodes. *Nano Energy* 2013;2:764-8. DOI
73. Wang C, Chui Y, Ma R, et al. A three-dimensional graphene scaffold supported thin film silicon anode for lithium-ion batteries. *J Mater Chem A* 2013;1:10092-8. DOI
74. Gupta KK, Li K, Balaji S, Kumar PS, Lu C. Microwave-assisted synthesis and electrochemical characterization of  $\text{TiNb}_2\text{O}_7$  microspheres as anode materials for lithium-ion batteries. *J Am Ceram Soc* 2023;106:4192-201. DOI
75. Zoller F, Peters K, Zehetmaier PM, et al. Making ultrafast high-capacity anodes for lithium-ion batteries via antimony doping of nanosized tin oxide/graphene composites. *Adv Funct Mater* 2018;28:1706529. DOI
76. Wang Y, Zhang Y, Li H, et al. Realizing high reversible capacity: 3D intertwined CNTs inherently conductive network for CuS as an anode for lithium ion batteries. *Chem Eng J* 2018;332:49-56. DOI
77. Örnek A. Positive effects of a particular type of microwave-assisted methodology on the electrochemical properties of olivine  $\text{LiMPO}_4$  (M= Fe, Co and Ni) cathode materials. *Chem Eng J* 2018;331:501-9. DOI
78. Sahu SR, Rikka VR, Haridoss P, Chatterjee A, Gopalan R, Prakash R. A novel  $\alpha\text{-MoO}_3$ /single-walled carbon nanohorns composite as high-performance anode material for fast-charging lithium-ion battery. *Adv Energy Mater* 2020;10:2001627. DOI
79. Tian Y, Liu X, Cao X, et al. Microwave-assisted synthesis of 1T  $\text{MoS}_2/\text{Cu}$  nanowires with enhanced capacity and stability as anode for LIBs. *Chem Eng J* 2019;374:429-36. DOI
80. Yin X, Chen X, Sun W, Lv L, Wang Y. Revealing the effect of cobalt-doping on Ni/Mn-based coordination polymers towards boosted Li-storage performances. *Energy Stor Mater* 2020;25:846-57. DOI
81. Cheng Y, Pandey RK, Li Y, et al. Conducting nitrogen-incorporated ultrananocrystalline diamond coating for highly structural stable anode materials in lithium ion battery. *Nano Energy* 2020;74:104811. DOI
82. Tang X, Wang H, Fan J, Lv L, Sun W, Wang Y. CNT boosted two-dimensional flaky metal-organic nanosheets for superior lithium and potassium storage. *Chem Eng J* 2022;430:133023. DOI
83. Zhou Y, Zhang X, Liu Y, et al. A high-temperature Na-ion battery: boosting the rate capability and cycle life by structure engineering. *Small* 2020;16:e1906669. DOI
84. Yao X, Ke Y, Ren W, et al. Defect-rich soft carbon porous nanosheets for fast and high-capacity sodium-ion storage. *Adv Energy Mater* 2019;9:1803260. DOI
85. Lu X, Wang Z, Liu K, et al. Hierarchical  $\text{Sb}_2\text{MoO}_6$  microspheres for high-performance sodium-ion battery anode. *Energy Stor Mater* 2019;17:101-10. DOI
86. Hou Y, Chang K, Wang Z, et al. Rapid microwave-assisted refluxing synthesis of hierarchical mulberry-shaped  $\text{Na}_3\text{V}_2(\text{PO}_4)_2\text{O}_2\text{F}@C$  as high performance cathode for sodium & lithium-ion batteries. *Sci China Mater* 2019;62:474-86. DOI
87. Martin A, Doublet M, Kemnitz E, Pinna N. Reversible sodium and lithium insertion in iron fluoride perovskites. *Adv Funct Mater* 2018;28:1802057. DOI

88. Guan J, Huang Q, Shao L, et al. Polyanion-type  $\text{Na}_3\text{V}_2(\text{PO}_4)_2\text{F}_3$ @rGO with high-voltage and ultralong-life for aqueous zinc ion batteries. *Small* 2023;19:e2207148. DOI
89. Zhao W, Fee J, Khanna H, et al. A two-electron transfer mechanism of the Zn-doped  $\delta\text{-MnO}_2$  cathode toward aqueous Zn-ion batteries with ultrahigh capacity. *J Mater Chem A* 2022;10:6762-71. DOI
90. Kim S, Soundharrajan V, Kim S, et al. Microwave-assisted rapid synthesis of  $\text{NH}_4\text{V}_4\text{O}_{10}$  layered oxide: a high energy cathode for aqueous rechargeable zinc ion batteries. *Nanomaterials* 2021;11:1905. DOI PubMed PMC
91. Jia D, Zheng K, Song M, et al.  $\text{VO}_2 \cdot 0.2\text{H}_2\text{O}$  nanocuboids anchored onto graphene sheets as the cathode material for ultrahigh capacity aqueous zinc ion batteries. *Nano Res* 2020;13:215-24. DOI
92. Chen S, Zhang Y, Geng H, Yang Y, Rui X, Li CC. Zinc ions pillared vanadate cathodes by chemical pre-intercalation towards long cycling life and low-temperature zinc ion batteries. *J Power Sources* 2019;441:227192. DOI
93. Xia C, Guo J, Lei Y, Liang H, Zhao C, Alshareef HN. Rechargeable aqueous zinc-ion battery based on porous framework zinc pyrovanadate intercalation cathode. *Adv Mater* 2018;30:1907798. DOI
94. Zhao T, Liu C, Meng T, et al. Vacancy-clusters in-situ induced via microwave-irradiation enable high-durability and capacitor-level rate li-ion storage. *Chem Eng J* 2023;466:143053. DOI
95. Jiang H, Xian J, Hu R, et al. Microwave discharge for rapid introduction of bimetallic-synergistic configuration to conductive catecholate toward long-term supercapacitor. *Chem Eng J* 2023;455:140804. DOI
96. Huang N, Sun Y, Liu S, et al. Microwave-assisted rational designed  $\text{CNT-Mn}_3\text{O}_4/\text{CoWO}_4$  hybrid nanocomposites for high performance battery-supercapacitor hybrid device. *Small* 2023;19:e2300696. DOI
97. Sun Y, Huang N, Zhao D, et al. Microwave-assisted in-situ isomorphism via introduction of Mn into  $\text{CoCo}_2\text{O}_4$  for battery-supercapacitor hybrid electrode material. *Chem Eng J* 2022;430:132729. DOI
98. Chen Y, Ni D, Yang X, Liu C, Yin J, Cai K. Microwave-assisted synthesis of honeycomblke hierarchical spherical Zn-doped Ni-MOF as a high-performance battery-type supercapacitor electrode material. *Electrochim Acta* 2018;278:114-23. DOI
99. Kaplan C, Hidalgo MFV, Zuba MJ, Chernova NA, Piper LFJ, Whittingham MS. Microwave-assisted solvothermal synthesis of  $\text{LiV}_y\text{M}_{1-y}\text{OPO}_4$  ( $\text{M} = \text{Mn, Cr, Ti, Zr, Nb, Mo, W}$ ) cathode materials for lithium-ion batteries. *J Mater Chem A* 2021;9:6933-44. DOI
100. Wan J, Huang L, Wu J, et al. Microwave combustion for rapidly synthesizing pore-size-controllable porous graphene. *Adv Funct Mater* 2018;28:1800382. DOI
101. Tian X, Cheng C, Qian L, et al. Microwave-assisted non-aqueous homogenous precipitation of nanoball-like mesoporous  $\alpha\text{-Ni}(\text{OH})_2$  as a precursor for NiOx and its application as a pseudocapacitor. *J Mater Chem* 2012;22:8029-35. DOI
102. Yan Z, Gao Z, Zhang Z, Dai C, Wei W, Shen PK. Graphene nanosphere as advanced electrode material to promote high performance symmetrical supercapacitor. *Small* 2021;17:e2007915. DOI PubMed
103. Chen T, Pan L, Lu T, Fu C, Chua DHC, Sun Z. Fast synthesis of carbon microspheres via a microwave-assisted reaction for sodium ion batteries. *J Mater Chem A* 2014;2:1263-7. DOI
104. Lai L, Zhu J, Li Z, et al.  $\text{Co}_3\text{O}_4$ /nitrogen modified graphene electrode as Li-ion battery anode with high reversible capacity and improved initial cycle performance. *Nano Energy* 2014;3:134-43. DOI
105. Amaresh S, Karthikeyan K, Jang I, Lee YS. Single-step microwave mediated synthesis of the  $\text{CoS}_2$  anode material for high rate hybrid supercapacitors. *J Mater Chem A* 2014;2:11099-106. DOI
106. Shi Y, Gao J, Abruña HD, et al. Rapid synthesis of  $\text{Li}_4\text{Ti}_5\text{O}_{12}$ /graphene composite with superior rate capability by a microwave-assisted hydrothermal method. *Nano Energy* 2014;8:297-304. DOI
107. Haruna AB, Barrett DH, Rodella CB, et al. Microwave irradiation suppresses the Jahn-Teller distortion in spinel  $\text{LiMn}_2\text{O}_4$  cathode material for lithium-ion batteries. *Electrochimica Acta* 2022;426:140786. DOI
108. Velásquez EA, Silva DPB, Falqueto JB, et al. Understanding the loss of electrochemical activity of nanosized  $\text{LiMn}_2\text{O}_4$  particles: a combined experimental and *ab initio* DFT study. *J Mater Chem A* 2018;6:14967-74. DOI
109. Karthikeyan K, Amaresh S, Aravindan V, Lee YS. Microwave assisted green synthesis of  $\text{MgO}$ -carbon nanotube composites as electrode material for high power and energy density supercapacitors. *J Mater Chem A* 2013;1:4105-11. DOI
110. Liu M, Zhao Q, Liu H, et al. Tuning phase evolution of  $\beta\text{-MnO}_2$  during microwave hydrothermal synthesis for high-performance aqueous Zn ion battery. *Nano Energy* 2019;64:103942. DOI
111. Lin F, Nordlund D, Weng TC, et al. Phase evolution for conversion reaction electrodes in lithium-ion batteries. *Nat Commun* 2014;5:3358. DOI
112. Ebner M, Marone F, Stampanoni M, Wood V. Visualization and quantification of electrochemical and mechanical degradation in Li ion batteries. *Science* 2013;342:716-20. DOI
113. Kim T, Park J, Chang SK, Choi S, Ryu JH, Song H. The current move of lithium ion batteries towards the next phase. *Adv Energy Mater* 2012;2:860-72. DOI
114. Kim H, Jegal J, Kim J, Yoon S, Roh KC, Kim K. In situ fabrication of lithium titanium oxide by microwave-assisted alkalization for high-rate lithium-ion batteries. *J Mater Chem A* 2013;1:14849-52. DOI
115. Sun Y, Li C, Yang C, et al. Novel  $\text{Li}_3\text{VO}_4$  Nanostructures grown in highly efficient microwave irradiation strategy and their in-situ lithium storage mechanism. *Adv Sci* 2022;9:e2103493. DOI PubMed PMC
116. Guo Y, Cao Y, Lu J, Zheng X, Deng Y. The concept, structure, and progress of seawater metal-air batteries. *Microstructures* 2023;3:2023038. DOI
117. Pei J, Chen G, Zhang Q, Bie C, Sun J. Phase separation derived core/shell structured  $\text{Cu}_{11}\text{V}_6\text{O}_{26}/\text{V}_2\text{O}_5$  microspheres: first synthesis

- and excellent lithium-ion anode performance with outstanding capacity self-restoration. *Small* 2017;13:1603140. DOI
118. Fan M, Liao D, Aboud MFA, Shakir I, Xu Y. A universal strategy toward ultrasmall hollow nanostructures with remarkable electrochemical performance. *Angew Chem Int Ed* 2020;59:8247-54. DOI
119. Liu K, Jin H, Huang L, et al. Puffing ultrathin oxides with nonlayered structures. *Sci Adv* 2022;8:eabn2030. DOI PubMed PMC
120. Yoon S, Manthiram A. Microwave-hydrothermal synthesis of  $W_{0.4}Mo_{0.6}O_3$  and carbon-decorated  $WO_x$ - $MoO_2$  nanorod anodes for lithium ion batteries. *J Mater Chem* 2011;21:4082. DOI
121. An G, Sohn JI, Ahn H. Hierarchical architecture of hybrid carbon-encapsulated hollow manganese oxide nanotubes with a porous-wall structure for high-performance electrochemical energy storage. *J Mater Chem A* 2016;4:2049-54. DOI
122. Cheng Q, Yang T, Li Y, Li M, Chan CK. Oxidation-reduction assisted exfoliation of  $LiCoO_2$  into nanosheets and reassembly into functional Li-ion battery cathodes. *J Mater Chem A* 2016;4:6902-10. DOI
123. Zhu J, Li Q, Bi W, et al. Ultra-rapid microwave-assisted synthesis of layered ultrathin birnessite  $K_{0.17}MnO_2$  nanosheets for efficient energy storage. *J Mater Chem A* 2013;1:8154-9. DOI
124. Zhao P, Li L, Wang X.  $BaTiO_3$ - $NaNbO_3$  energy storage ceramics with an ultrafast charge-discharge rate and temperature-stable power density. *Microstructures* 2022;3:2022023. DOI
125. Lee K, Shin S, Degen T, Lee W, Yoon YS. In situ analysis of  $SnO_2/Fe_2O_3/RGO$  to unravel the structural collapse mechanism and enhanced electrical conductivity for lithium-ion batteries. *Nano Energy* 2017;32:397-407. DOI
126. Sridhar V, Kim HJ, Jung JH, Lee C, Park S, Oh IK. Defect-engineered three-dimensional graphene-nanotube-palladium nanostructures with ultrahigh capacitance. *ACS Nano* 2012;6:10562-70. DOI
127. Lee SH, Sridhar V, Jung JH, et al. Graphene – nanotube - iron hierarchical nanostructure as lithium ion battery anode. *ACS Nano* 2013;7:4242-51. DOI
128. Wang X, Wang Y, Wu M, Fang R, Yang X, Wang D. Ultrasonication-assisted fabrication of porous  $ZnO@C$  nanoplates for lithium-ion batteries. *Microstructures* 2022;2:2022016. DOI
129. Li D, Guo Q, Cao M, Yao Z, Liu H, Hao H. The influence of A/B-sites doping on antiferroelectricity of PZO energy storage films. *Microstructures* 2023;3:2023007. DOI
130. Dai R, Sun W, Lv LP, et al. Bimetal-organic-framework derivation of ball-cactus-like Ni-Sn-P@C-CNT as long-cycle anode for lithium ion battery. *Small* 2017;13:1700521. DOI
131. Wang Y, Ke J, Zhang Y, Huang Y. Microwave-assisted rapid synthesis of mesoporous nanostructured  $ZnCo_2O_4$  anode materials for high-performance lithium-ion batteries. *J Mater Chem A* 2015;3:24303-8. DOI
132. Nayak PK, Yang L, Brehm W, Adelhelm P. From lithium-ion to sodium-ion batteries: advantages, challenges, and surprises. *Angew Chem Int Ed* 2018;57:102-20. DOI PubMed
133. Zhao C, Lu Y, Li Y, et al. Novel methods for sodium-ion battery materials. *Small Methods* 2017;1:1600063. DOI
134. Yang Q, Fan Q, Peng J, Chou S, Liu H, Wang J. Recent progress on alloy-based anode materials for potassium-ion batteries. *Microstructures* 2023;3:2023013. DOI
135. Yabuuchi N, Kubota K, Dahbi M, Komaba S. Research development on sodium-ion batteries. *Chem Rev* 2014;114:11636-82. DOI PubMed
136. Roh H, Kim H, Kim M, et al. In situ synthesis of chemically bonded  $NaTi_2(PO_4)_3/rGO$  2D nanocomposite for high-rate sodium-ion batteries. *Nano Res* 2016;9:1844-55. DOI
137. Sengupta A, Kumar A, Barik G, et al. Lower diffusion-induced stress in nano-crystallites of  $P_2-Na_{2/3}Ni_{1/3}Mn_{1/2}Ti_{1/6}O_2$  novel cathode for high energy Na-ion batteries. *Small* 2023;19:e2206248. DOI
138. Jin H, Song T, Paik U, Qiao SZ. Metastable two-dimensional materials for electrocatalytic energy conversions. *Acc Mater Res* 2021;2:559-73. DOI
139. Islam S, Lee S, Lee S, et al. Triggering the theoretical capacity of  $Na_{1.1}V_3O_{7.9}$  nanorod cathode by polypyrrole coating for high-energy zinc-ion batteries. *Chem Eng J* 2022;446:137069. DOI
140. Liu L, Lin Z, Shi Q, et al. High-performance 3D biphasic  $NH_4V_3O_8/Zn_3(OH)_2V_2O_7 \cdot 2H_2O$  synthesized by rapid chemical precipitation as cathodes for Zn-ion batteries. *Electrochem Commun* 2022;140:107331. DOI
141. Wang G, Zhang L, Zhang J. A review of electrode materials for electrochemical supercapacitors. *Chem Soc Rev* 2012;41:797-828. DOI
142. Luo Q, Lu C, Liu L, Zhu M. Triethanolamine assisted synthesis of bimetallic nickel cobalt nitride/nitrogen-doped carbon hollow nanoflowers for supercapacitor. *Microstructures* 2023;3:2023011. DOI
143. Liu G, Chen L, Qi H. Energy storage properties of  $NaNbO_3$ -based lead-free superparaelectrics with large antiferrodistortion. *Microstructures* 2023;3:2023009. DOI
144. Simon P, Gogotsi Y, Dunn B. Materials science. Where do batteries end and supercapacitors begin? *Science* 2014;343:1210-1. DOI PubMed
145. Wang W, Xiao Y, Li X, Cheng Q, Wang G. Bismuth oxide self-standing anodes with concomitant carbon dots welded graphene layer for enhanced performance supercapacitor-battery hybrid devices. *Chem Eng J* 2019;371:327-36. DOI
146. Wang W, Jin J, Wu Y, et al. Unique holey graphene/carbon dots frameworks by microwave-initiated chain reduction for high-performance compressible supercapacitors and reusable oil/water separation. *J Mater Chem A* 2019;7:22054-62. DOI
147. Sun Y, Zhang J, Liu S, Sun X, Huang N. An enhancement on supercapacitor properties of porous CoO nanowire arrays by microwave-assisted regulation of the precursor. *Nanotechnology* 2021;32:195707. DOI

148. Jiang Y, Guo S, Li Y, Hu X. Rapid microwave synthesis of carbon-bridged Nb<sub>2</sub>O<sub>5</sub> mesocrystals for high-energy and high-power sodium-ion capacitors. *J Mater Chem A* 2022;10:11470-6. [DOI](#)
149. Wang Z, Jia W, Jiang M, Chen C, Li Y. Microwave-assisted synthesis of layer-by-layer ultra-large and thin NiAl-LDH/RGO nanocomposites and their excellent performance as electrodes. *Sci China Mater* 2015;58:944-52. [DOI](#)
150. Lin L, Yeh M, Tsai J, Huang Y, Sun C, Ho K. A novel core-shell multi-walled carbon nanotube@graphene oxide nanoribbon heterostructure as a potential supercapacitor material. *J Mater Chem A* 2013;1:11237. [DOI](#)
151. Gupta N, Sahu RK, Mishra T, Bhattacharya P. Microwave-assisted rapid synthesis of titanium phosphate free phosphorus doped Ti<sub>3</sub>C<sub>2</sub> MXene with boosted pseudocapacitance. *J Mater Chem A* 2022;10:15794-810. [DOI](#)
152. Wang W, Zhang W, Wang G, Li C. Electrophoresis-microwave synthesis of S,N-doped graphene foam for high-performance supercapacitors. *J Mater Chem A* 2021;9:15766-75. [DOI](#)